Influence of the laser ablation surface pre-treatment over the ageing resistance of metallic adhesively bonded joints

Influence of the laser ablation surface pre-treatment over the ageing resistance of metallic adhesively bonded joints

F. Moroni[1], F. Musiari[1]*, C. Favi[1]

[1]Università degli Studi di Parma, Dipartimento di Ingegneria e Architettura, Parco Area delle Scienze, 181/A, 43124 Parma, IT.

In order to prevent the generation of a potential weakness at the substrate/adhesive interface of adhesively bonded joints, many methods were developed during the decades to pre-treat the substrates surfaces before the deposition of the adhesive. Experimental tests were carried out to simulate the real environmental conditions in which the joints have to work characterizing the mechanical properties of the joints caused by the exposition to high temperature, moisture, presence of chemical agents. The industrial need towards long-scale problem lead to the development of specific accelerated ageing methods able to induce in few weeks the same damage mechanisms within the joints which arise in years during their working life. In this work, different surface laser pre-treatments were studied with a focus on the influence that pre-treatments produce over the variation of the tensile failure load of Single Lap Joints (SLJ), previously subjected to different accelerated ageing cycles. Simple degreasing and grit blasting were also considered as reference treatments. The materials chosen for the manufacturing of the substrates were an aluminium alloy (AA 6082-T6) and a stainless steel (AISI 304). Three different accelerated ageing techniques were tested and compared to each other: (i) a cycle involving the simultaneous presence of high temperature gradient and moisture (method A), (ii) the immersion into an alkaline foam-forming cleanser (method B), and (iii) the immersion into an acid foam-forming cleanser (method C). The results showed that, while the method A did not significantly modify the mechanical strength of the joints, the method B and C resulted detrimental for the mechanical performance of the joints, even if their sensitivity to the tested pre-treatments was different. In particular, for both aluminum and stainless steel joints, it was noticed that the laser pre-treatment was able to reduce the loss of strength produced by the ageing process in comparison with the two reference pre-treatments. However, this result was also dependent of the specific value of energy density used for the laser ablation during the joints pre-treatment.

*Corresponding author – e.mail: francesco.musiari@unipr.it

Keywords: Ageing, Surface Treatment, Laser ablation, Aluminum, Stainless Steel

1 Introduction

Adhesive bonding is a joining method increasingly used in several branches of the manufacturing industry. The advantages brought with respect to other traditional methods are wide, from the possibility to have lighter structures without detriment of the strength to the possibility to avoid hole's realization for the connection of the components. This last aspect is particularly important for those structures that require the reduction of the stress concentrations occurring instead using other assembly processes such as nailing, screwing or, to a lesser extent, welding [1]. On the other hand, two main issues penalise the goodness of adhesive bonding with respect to other joining methods: (i) the need to adequately prepare the surfaces to be bonded in order to avoid the formation of weak boundary layers, and (ii) the difficulty to reliably characterize the real working conditions of the bonded structures during their service life. With respect to the first issue, the beneficial effects provided to the strength of joints thanks to the capability of several pre-treatments to modify both the surface morphology and the wettability were extensively documented. As provided in many research works, both chemical (e.g. degreasing [2], etching [3-5], chemical anodizing [6-7]) and mechanical (e.g. grit blasting [8-9], abrasion [10], plasma spray coating [11]) methods were tested demonstrating their benefits. In particular, these works aim at the characterization of a link between the process conditions, which include the substrate material and the adhesive, and the mechanical strength of the adhesively bonded joints remarking how the failure mode switches from interfacial to cohesive (i.e. within the adhesive, as it is desirable). With respect to the second issue, the environmental conditions in which the bonded structures work play a crucial role in determining the strength and the resistance of the joints to the applied loads. Indeed, the exposure to high temperatures and levels of moisture, as well as the presence of aggressive atmospheres, usually lead to a worsening of the mechanical performance of the joins, often accompanied by a change of the failure mode from cohesive to adhesive [12-13]. The need for the industry to collect reliable data in reasonable times makes difficult to reproduce the environmental exposure actually experimented by the joint during the real working conditions, whose associated degrading phenomena usually last years to fully develop. For this reason, accelerated ageing methods were developed, with the intent to induce the same effects obtainable after years of environmental aggression in a more confined time. The influence of many process variables over the ageing resistance of adhesively bonded joints were studied in the past. Concerning the wide range of available pre-treatments, the chemical ones were found to give better results than the mechanical ones [14]. However, some inconsistencies of the inner ranking between different treatments (e.g. phosphoric acid anodizing or sulfuric-chromic acid etching vs. chromic acid anodizing) were detected [14-15]. Costa *et al* [16] considered the response provided by the joints in presence of

moisture and depending from the type of adhesive employed. They compared to each other a brittle and a ductile adhesive by immersing bulk specimens and Double Cantilever Beam (DCB) aluminium joints in distilled water at 32°C and by measuring the variation in the stress-strain response and in the fracture toughness in function of the exposure time. The brittle adhesive was found to suffer a more accentuated decrease of the mechanical properties with respect to the unaged conditions, while in the ductile adhesive the water absorption was lower than in the other case, resulting only in a higher elongation at break which made the fracture toughness rise up with respect to the unaged value. Viana *et al* [17] studied the changing in the glass transition temperature (Tg) of the same two adhesive systems in presence of two different aggressive atmospheres (namely distilled water and a saturated solution of NaCl) coupled with three different temperatures (ranging from -40°C to 80°C). Even in this case, the brittle adhesive presented a more severe decrease of Tg than the ductile adhesive, especially when exposed to distilled water which was identified as the most aggressive environment among the tested ones.

With specific refer to the laser ablation, some works explored its capability to keep unmodified the induced changings of the surface morphology, and therefore of the mechanical behavior, after an environmental exposure. In [18], Rechner *et al* evaluated the variation of the shear strength of aluminium/epoxy SLJs, which were exposed to a salt spray atmosphere for several hours and were previously pre-treated using a Nd:YAG laser (wavelength λ=1064 nm, mean output power P=0-120 W, continuous frequency range f=8-40 kHz, pulse maximum power P_{MAX}=120 kW, range of processing speeds v=0-4000 mm/s) with different intensities (5 levels from 1.73 x 10^{11} W/m^2 to 4.42 x 10^{11} W/m^2) obtained by varying the pulse frequencies and keeping the power and the scan speed fixed. The laser ablation treatment was found to be capable to increase the shear strength of the aged joints with respect to the untreated case by a factor equal to 26% and 15% after 1000 and 2000 exposure hours, respectively. The failure mode after 1000 hours of ageing consistently switched from completely adhesive in the untreated joints to predominately cohesive in the laser ablated specimens. Wu *et al* [19] tested aluminium SLJs after performing laser ablation with different process parameters combinations over the substrates surface and after immersing the joints into water at 54°C for 7 days. When the laser fluence overstepped a threshold, the ablation succeeded in limiting the decrease of the shear strength after the water soak with respect to the unaged conditions.

In this work, several pre-treatments were applied over the surfaces of substrates realized both in aluminium and in stainless steel: (i) degreasing, (ii) grit blasting, and (iii) laser ablation. The final goal of this work is to compare their effect over the variation of the failure load of Single Lap Joints

(SLJs) realized with them and undergone different accelerated ageing cycles. Several laser ablation configurations obtained by varying some process parameters were experimented, exploiting the best results already identified in a previous work [20]. This work is aimed to study the suitability of the laser treatment as adhesion promoter for adhesively bonded connection in the field of the food machines construction. Therefore, the ageing conditions considered were selected accordingly. In particular, three different accelerated ageing techniques were tested and compared to each other: (i) a cycle involving the simultaneous presence of high temperature gradient and moisture (method A), (ii) the immersion into an alkaline foam-forming cleanser (method B), (iii) the immersion into an acid foam-forming cleanser (method C). Both the alkaline and the acid cleanser were commonly employed in the cleaning process of machine and equipment used in the food industry, justifying the adoption of these cleansers.

2 Experimental setup

2.1 Materials and geometry

Two materials were considered for the production of the substrates employed to assemble the joints used for the experimental tests, namely AA6082-T6 aluminium alloy and AISI 304 stainless steel. The mechanical properties of the two selected materials are provided in Table 1.

Table 1 - Mechanical properties of the materials used for the joints production (taken from supplier certificate)

Material	AA6082-T6	AISI 304
Young modulus E_s	70 GPa	190 GPa
Poisson's ratio ν_s	0.33	0.29
Tensile Yield Strength Rp_s	295 MPa	230 MPa
Tensile Ultimate Strength Ru_s	320 MPa	510 MPa

A toughened two-component epoxy adhesive - Loctite Hysol 9466 - (whose properties are listed in Table 2) was used to bond the substrates together.

Table 2 - Loctite Hysol 9466 mechanical properties (taken from www.henkel.com)

Young modulus E_a	1718 MPa
Poisson's ratio ν_a	0.35
Tensile Ultimate Strength Ru_a	32 MPa

The chosen geometry for the test was the Single Lap-shear Joint (SLJ) in order to detect the influence of the employed pre-treatment over the possible decrease of the failure load induced by the ageing conditions. Figure 1 illustrates the dimensions of the produced joints, which are summarised in Table 3.

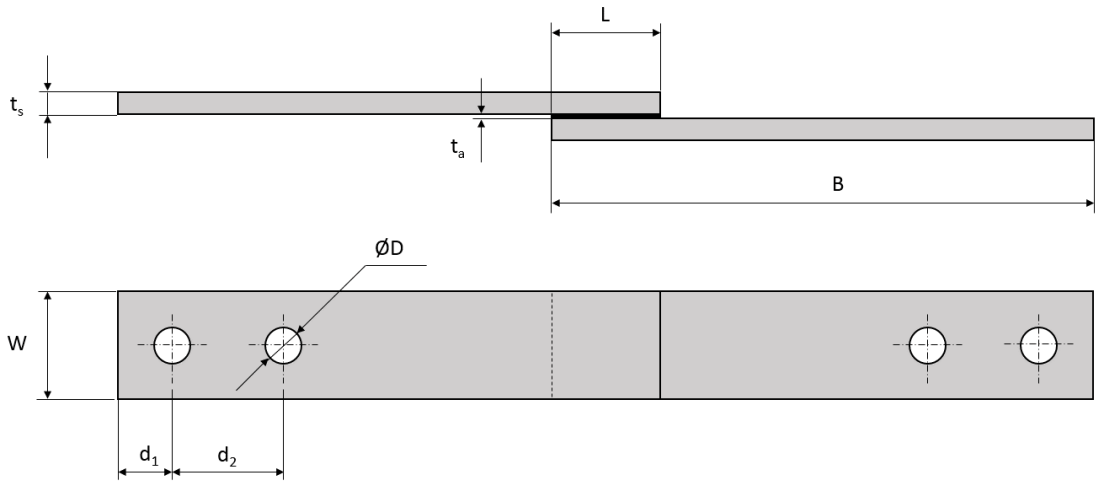

Figure 1 – SLJ geometry

Table 3 - SLJ dimensions

W (mm)	B (mm)	D (mm)	d_1 (mm)	d_2 (mm)	t_s (mm)	t_a (mm)	L (mm)
25	90	8	7.5	24	3	0.2	15

2.2 Joint preparation

After cleaning operation of the substrates with water and soap with the aim to remove the traces of residual contaminants eventually coming from the manufacturing, the substrates were subjected to several pre-treatments before the deposition of the adhesive occurred. In particular, three methods were compared to each other with respect to the capability to minimize the effect of the environmental exposure over the mechanical response:

1. *Degreasing*: the substrate surfaces were simply cleansed with Henkel 7063 chemical degreaser*;*
2. *Grit blasting*: the substrate surfaces were treated with a grit blasting process employing alumina particles (grade 80) at a pressure of 0.5 MPa and at a distance approximately equal

to 30 mm from the nozzle and finally cleansed with the same product used to perform the simple degreasing;

3. *Laser ablation:* the substrate surfaces were ablated by means of a pulsed Yb-fiber laser, featuring a z-axis positioning system for focus adjustment and a x-y galvo-mirror scanner, and by properly selecting some specific combinations of process parameters. The available process parameters are listed in Table 4.

Table 4 - Process parameters of the laser equipment

Laser nominal average power P_{AVE}	0-20 W
Laser radiation wavelength λ	1055-1070 nm
Pulse repetition frequency f_r	20-80 kHz
Emission linewidth	<10 μm
Mode of operation	Pulsed
Minimum pulse FWHM	120 ns

In reference to the last method, the adopted configurations to perform the ablation were chosen according to the results of some previous experimental campaigns described in [21]. In particular, the index assumed as representative of the specific combination of process parameters employed was the energy density, defined as in Eq. (1).

$$ED = \frac{P}{v\Phi_s} \quad (1)$$

In Eq. (1), P is the average lasing power, v is the tangential scan speed and Φ_s is the nominal diameter of the laser induced single spot, kept fixed to 35 μm. In addition to these parameters, the effect of the hatch distance (H), defined as the nominal distance between two adjacent laser induced grooves, was evaluated, while the pulse repetition frequency (f) was maintained to 20 kHz. The levels of energy density to perform the ablation were selected in order to explore the whole range of mechanical behaviors detected in [21] by means of Double Cantilever Beam (DCB) tests. These values allowed to define a wide range of failures, from an interfacial failure for very low values of ED, to a completely cohesive failure and extremely high toughness induced by somemedium values of ED and finally to a failure which, although remaining macroscopically cohesive, was affected by the presence of air inclusions remained trapped within the very deep grooves resulting from high

levels of ED.. Four ED values were used to carry out the pre-treatment: (i) low value (ED = 0.17 J/mm^2), (ii) medium-low value (ED = 0.51 J/mm^2) (iii) medium-high value (ED = 1.14 J/mm^2) and (iv) high value (ED = 5.71 J/mm^2). The influence of a variation of the hatch distance H from 50 to 100 μm was evaluated only for the ED = 0.51 J/mm^2 set, while for the other classes of specimens its value was kept fixed to 50 μm.

After the performance of the pre-treatment, the substrates were bonded together and the curing cycle occurred at 80°C for one hour in a controlled climatic chamber, consistently with the supplier prescriptions.

2.3 Environmental exposure conditions

In this work, three different methods were employed to recreate some critical environmental conditions which the bonded joints usually can undergo during their working life and to allow to speed up the process of getting information about the mechanical response of the aged joints. One of these methods (A) involved the simultaneous application of temperature and moisture gradients, while the other two techniques consisted in immersing the joints into two solutions, one alkaline (B) and one acid (C), respectively. The choice of the ageing method A was due to the suitability of the explored ranges of temperature and moisture to the ones possibly encountered during the service life. The cycle did not prescribe extreme levels of temperature and moisture which was in line with the statement by Adams [22] dealing with the fact that too high temperature and moisture levels usually trigger damage mechanisms which were poorly representative of the real conditions of the joints. Indeed, with reference to methods B and C, the selected products were among a series of products under assessment for being employed for practical applications (e.g.: for sanitizing or sterilizing) in some companies belonging to the food machine industry field which commonly use adhesively bonded joints. In the following a brief description of each technique will be provided.

The method (A) corresponds to the accelerated ageing cycle D3 referred in the international standard DIN ISO 9142 and it was performed within an ACS – DY110 environmental test chamber (ACS, Massa Martana, Italy). Initially the cycle required that samples underwent a preliminary conditioning for 24 h at a temperature of 23°C and at a relative humidity RH of 50%. Then the repeated application of the following six steps, represented in Figure 2, was needed:

a) exposure for 15 h at a temperature of 40°C and a relative humidity of 90%
b) change in 60 min to a temperature of -20°C
c) exposure for 2 h at a temperature of -20°C
d) change in 60 min to a temperature of 70°C and to a relative humidity of 50%

e) exposure for 4 h at a temperature of 70°C and a relative humidity of 50%

f) change in 60 min to a temperature of 40°C and a relative humidity of 90%

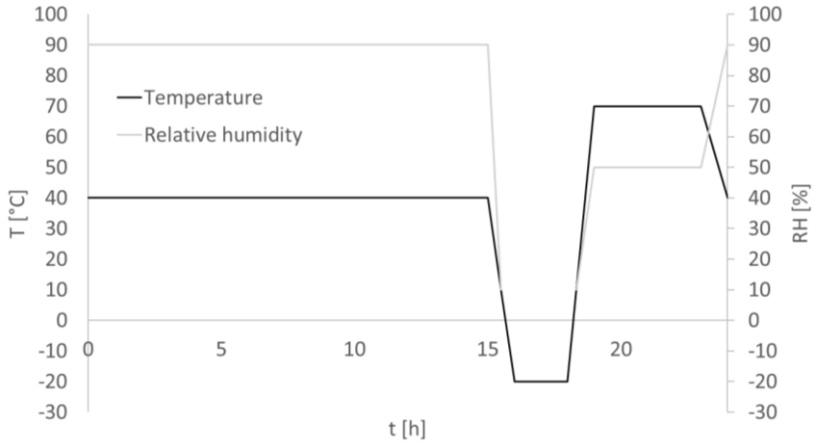

Figure 2 - Accelerated ageing cycle D3 according to DIN ISO 9142

The humidity control was disabled before reaching the freezing point and until the temperature did not return to 10°C during the subsequent ascending step. The total ageing time was set to 8 weeks, in order to try to amplify the effect already tested in [20] when the same cycle was applied over DCB joints for 4 weeks, consistently with what documented in literature [23,24].

The methods (B) and (C) consisted in immersing the specimens within two solutions, alkaline and acid, respectively. In particular, the method (B) required to maintain the joints into a 2% v/v solution of P3-Topactive LA in deionized water, at 70°C, for 72 hours, which was approximately corresponding to 15 minutes/week of industrial washing for 5 years. Instead, the method (C) consisted in an immersion of the samples into a 5% v/v solution of EnduroEco VE9 in deionized water, at room temperature, for 16 days, which was a time equal to the one required by a common industrial cleansing lasting 30 minutes/week, repeated for 15 years. Table 5 provides some additional details about the two employed solutions.

Table 5 – Detailed features of the chemical agents (taken from supplier data sheets)

Solution	Density [g/cm^3]	pH	Active ingredients (>1%)
P3-Topactive LA	1.10-1.14	10.7 – 11.0 (1%, 20°C, deionized water)	Ethanol Sodium carbonate D-Glucopyranose, oligomeric, C10-16 alkyl glycosides Acids D-Glucopyranose, oligomeric, decyl octyl glycosides
Enduro Eco VE9	1.21	ca. 2 (1%, 20°C, deionized water)	Phosphoric acid Propan-2-ol Oleyl bis(2-hydroxyethyl)amine Sodium xylene sulphonate N,N-dimethyltetradecylamine-oxide

2.4 Mechanical characterization

A series of quasi-static tensile tests was used to assess the failure load of the different pre-treated SLJs. After being removed from the cycle which they were subjected to, the specimens were made rest for 1 hour at room temperature and then they were tested under the same environmental conditions in a MTS 810 servo-hydraulic machine (MTS Systems, Torino, Italy), equipped with a 100 kN load cell, in displacement control (1.3 mm/min), according to ASTM D1002. Four specimens were tested for each pre-treatment for every ageing condition. Test were performed at a temperature of 23±3°C and a relative humidity of 50±10%.

3 Results

3.1 Aluminium joints

Figure 3 depicts the mechanical behavior resulting from the assessment of the failure load of the differently pre-treated joints realized with aluminium substrates. The height of the rectangles represents the mean failure load evaluated from the totality of the tested specimens of a class, while the bars represent the standard deviation.

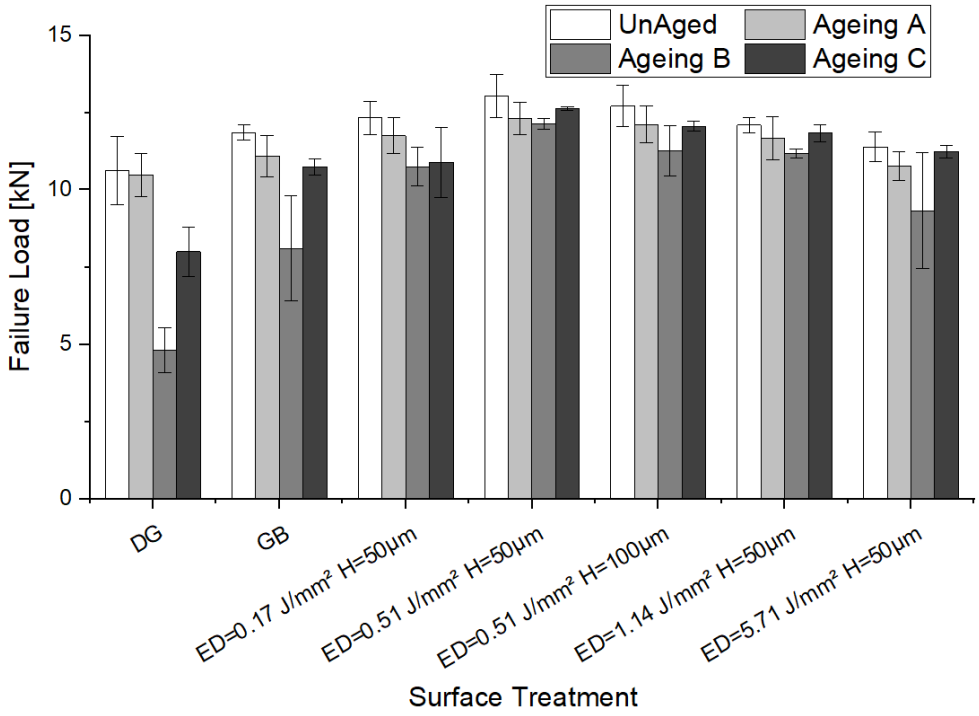

Figure 3 –Effect of the ageing over the failure load of the aluminium SLJs pre-treated with different methods: degreasing (DG), grit blasting (GB) and laser ablation using several values of energy density (ED) and hatch distance (H).

Firstly, looking at the whole data set, it is possible to notice how for every class of specimens distinguished according to the employed pre-treatment, regardless of the presence and the type of the ageing process, the mean value of the failure load appeared to increase moving from the degreased (DG) to the grit blasted (GB) and finally to the laser ablated samples processed with low values of ED. In the unaged case, the mean amount of the increase of the failure load value with respect to the degreased samples was equal to 11.5% in the grit blasted joints, while the strengthening effect provided by the laser ablated specimens ranged from +7.2% (for the highest ED family) to +22.7% (for the ED=0.51 J/mm^2 and H=50 µm group, which marked a threshold in the failure load trend. Considering the influence that the tested ageing process had over the mechanical response, Figure 4 provides a useful frame. This graph addresses the extension of the decrease exhibited by the failure load of the aged specimens with respect the one of the unaged joints, being fixed the applied pre-treatments. By looking to the simple degreased joints some peculiarities appeared evident: (i) the ageing method (A) did not seem to significantly alter the mechanical properties of the joints, (ii) the samples treated with the method (B) show a remarkable detrimental effect able to drop down the failure load up to -55% with respect to the unaged value

and, (iii) the aging method (C) shows the same behavior of the method (B) with a slightly lesser extent (approx. -25% than the corresponding unaged property).

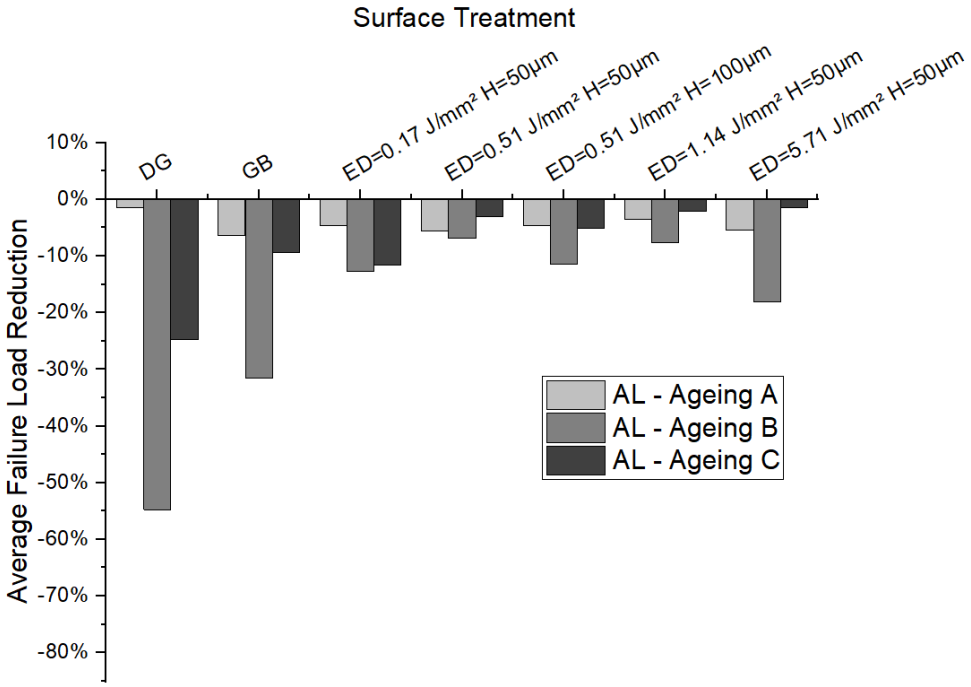

Figure 4 -Influence of the ageing method over the average failure load reduction of aluminium SLJs, diversified according to the applied pre-treatment

The reduction of the failure load recorded when the ageing method (A) was applied became more relevant (about -5%) in the grit blasted case and it remained approximately constant to this level in all the laser ablated joints, regardless of the combinations of parameters employed. Instead, for the grit blasted case both the other two considered ageing techniques resulted in a lesser effect over the failure load with respect to the unaged conditions: the decrease of the failure load with respect to the unaged value was about 30% and 10%, for the joints treated with method (B) and (C), respectively. The differences of mechanical behavior induced by the different ageing method applied were however evident by comparing to each other the fracture surfaces of the grit blasted joints, which are presented in Figure 5. Although the fracture locus appeared predominantly confined to the interface, the appearance of the adhesive side switched from being quite indented (in the unaged and aged with method A cases) to resulting completely smooth (when the ageing was performed according to method B or C), pointing out that a completely adhesive failure presumably occurred.

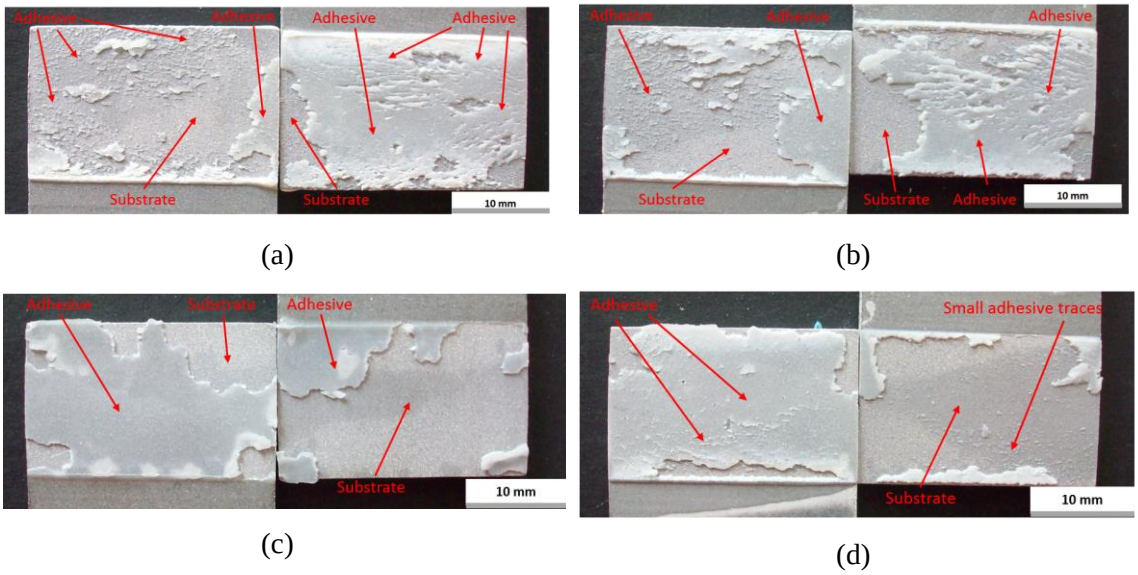

Figure 5 – Photographs showing details of fracture surface of aluminium SLJs pre-treated with grit blasting and subjected to different ageing methods: (a) unaged; (b) method (A); (c) method (B); (d) method (C)

In order to provide an additional evidence, some SEM analysis were carried out on the fracture surfaces, respectively for method (A) (Figure 6), method (B) (Figure 7), and method (C) (Figure 8). In Figure 6, the presence of residual adhesive on corresponding places of the fracture surfaces of the two substrates of a grit blasted specimen subjected to D3 cycle (method A) is evident. Indeed, even on the substrate where the crack propagated close to the interface, a thin layer of adhesive was detected (Figure 6(i)). Moreover, from Figure 6(ii), several stacked layers of adhesive are visible as a result of the crack propagation, which is typical of a cohesive failure. Figure 7 shows a SEM acquisition of a fracture surface of a grit blasted specimen aged with method (B): in Figure 7(i), the morphology of the aluminum matrix is appreciable, while in Figure 7(ii) only epoxy adhesive is present (including the presence of air remained entrapped within the adhesive during the cure). Additional EDX spectra evaluated on the whole observed surface are provided in Figure 8, pointing out the occurrence of a predominantly adhesive fracture. Finally, Figure 9 presents the results of a SEM morphological analysis performed on a grit blasted joint subjected to aging method (C): the fracture is confirmed to be predominantly interfacial, even if some portions of detached adhesive were actually found on the substrate where bare aluminum is visible (Figure 9(ii)). As outcome, the EDX measurements (Figure 10) confirmed the SEM acquisitions.

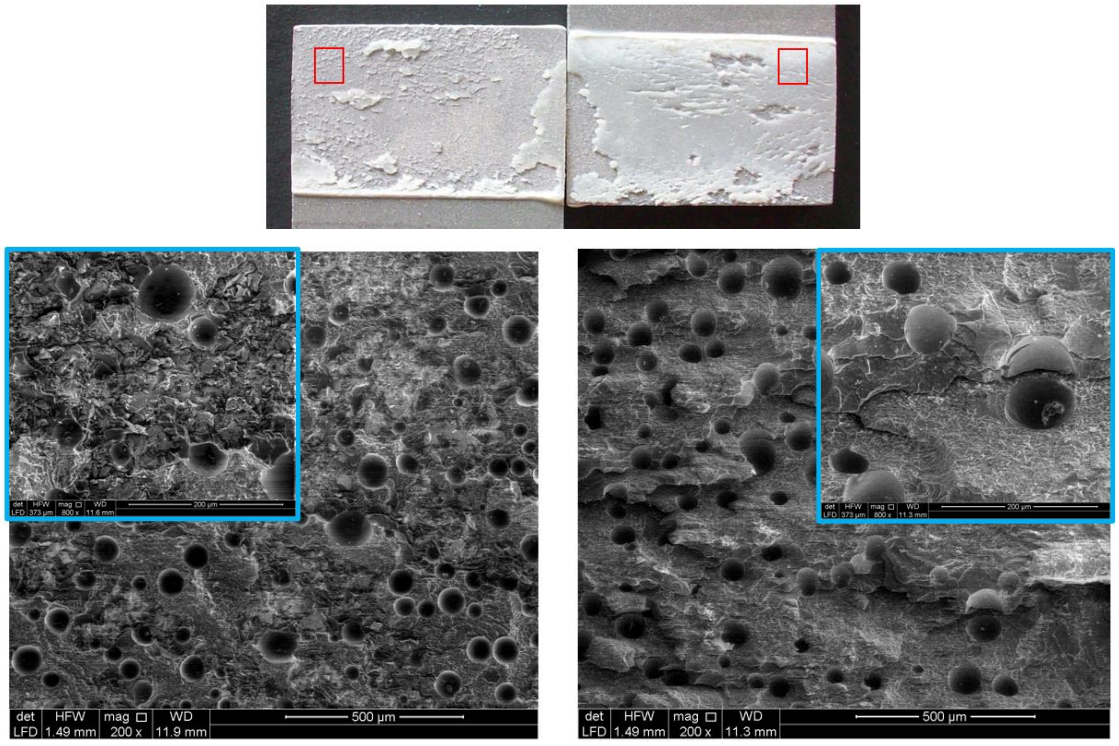

(i) (ii)

Figure 6 - SEM images of fracture surface of grit blasted aluminum joint subjected to method A ((i) left side; (ii) right side), with magnified details (in the blue boxes)

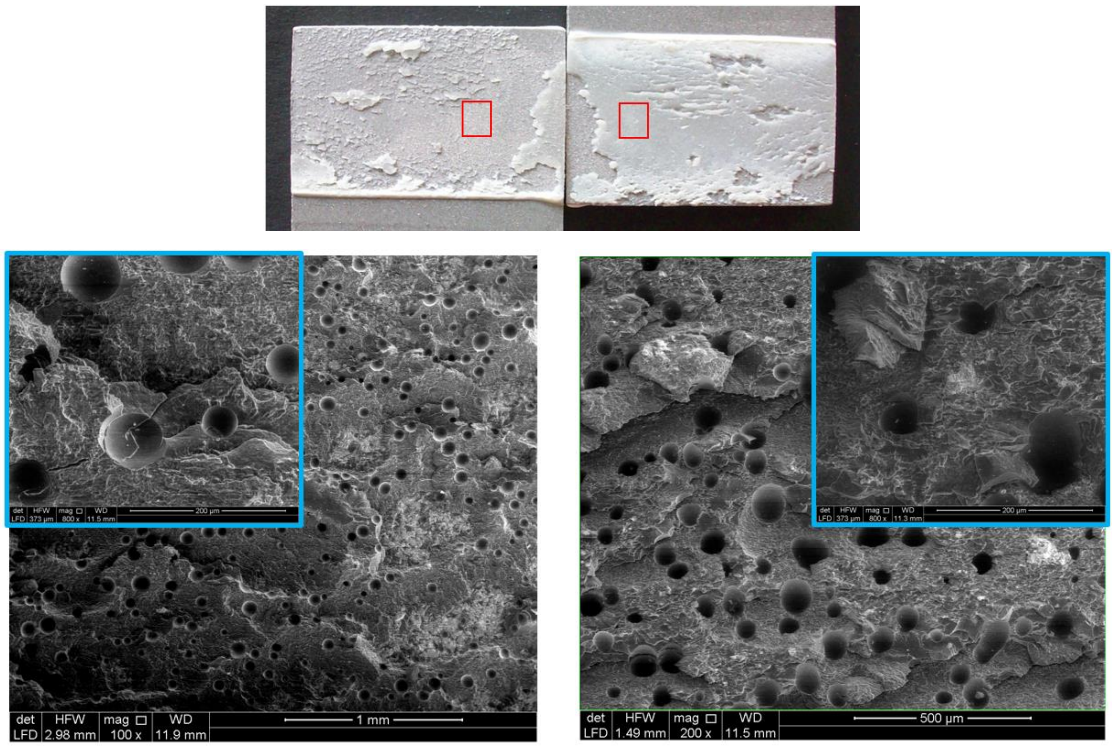

(i) (ii)

Figure 7 - SEM images of fracture surface of grit blasted aluminun joint subjected to method B ((i) left side; (ii) right side), with magnified details (in the blue boxes)

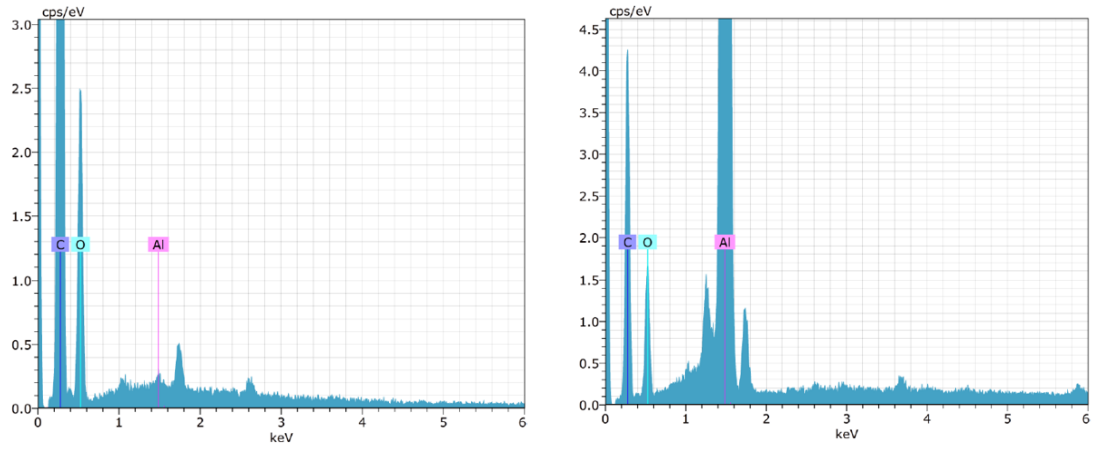

(i) (ii)

Figure 8 - Global EDX spectra measured on the observed surface shown in Figure 7(i) and (ii), respectively

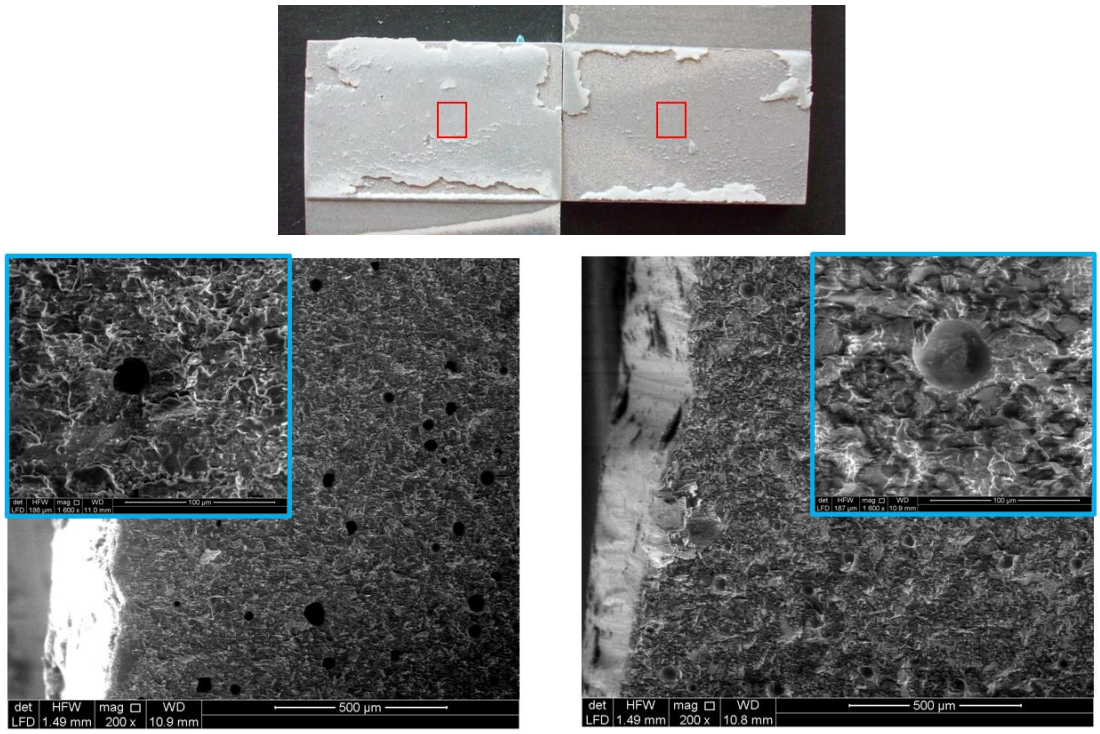

(i) (ii)

Figure 9 - SEM images of fracture surface of grit blasted aluminum joint subjected to method C((i) left side; (ii) right side), with magnified details (in the blue boxes). The cut appearing on a side of the process area is due to the need for the samples to be machined in order to be properly analyzed with SEM apparatus

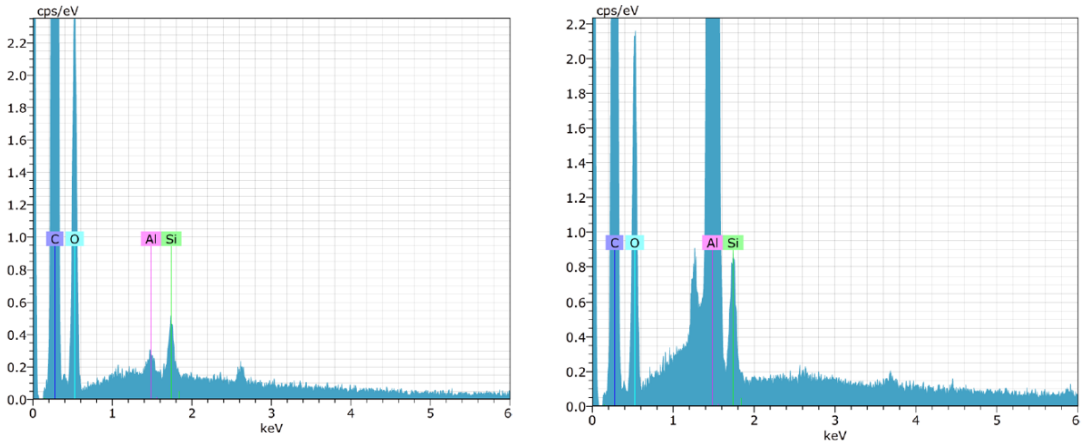

(i) (ii)

Figure 10 - Global EDX spectra measured on the observed surface shows in Figure 9(i) and (ii), respectively

With regard to the laser ablated joints, the treatment seemed to be capable to considerably reduce the sensitivity of the mechanical performance to the ageing conditions, when they involved the immersion into the tested cleansers. Keeping the hatch distance fixed to 50 µm, an increase of ED from 0.17 J/mm^2 to 0.51 J/mm^2 triggered a decline in the reduction of the failure load compared to

the unaged result from approximately 13% to 7% when method (B) was used and from about 12% to 3% in the joints undergoing ageing with method (C). Nevertheless, even when the values appeared very close to each other, different failure modes occurred according to the considered class of specimens. The fracture analysis reported in Figure 11 shows the samples belonging to the set characterized by ED = 0.51 J/mm^2 and H = 50 μm. In the unaged joints, the surface presented a predominantly cohesive fracture and the crack path resulted very jagged along the whole bonded region (Figure 11 (a)). The failure mode associated to the ageing (A) was reported in Figure 11 (b) and, although it was quite similar to the one of the unaged samples, the amount of area interested in a more interfacial failure was increased with respect to the previous case, which was consistent with the mechanical results. The failure apparently became predominantly adhesive when treating the specimens with ageing method (B) (Figure 11 (c)), which pointed out the higher reduction of failure load recorded for this set of specimens with respect to the unaged one. Finally, the unwinding of the failure load detected for the joints aged with method (C) found evidence in a return to a more indented crack path and an increase of the portion of area affected by a cohesive failure (Figure 11 (d)). In order to investigate the differences between the fracture modes associated to different aging methods, being equal the process conditions, SEM morphological observations are performed on the same specimens showed in Figure 11. From Figure 12, the fracture surface of the unaged joint actually appears predominantly covered by adhesive. This adhesive prevalence is also confirmed by additional EDX measurements (Figure 13) performed on the same sites of the morphological observation, even if some traces of aluminum were however detected, probably due to Al_2O_3 powders abraded by laser and left on the substrates. Analyzing the sample subjected to aging method B (Figure 14), the appearance of the SEM images confirms the visual analysis, nevertheless some traces of adhesive resulted spare over the surface (as it is shown in the box in Figure 14(ii)), which is confirmed from EDX measurements (Figure 15). Even in this case, the presence of aluminum found in the adhesive zone can be traced back to the residual ablated powders. Finally, on the fracture surface of the joint subjected to method C, the areas on which the aluminum substrate appears barely visible are actually characterized by alternation with adhesive zones (Figure 16). In particular, while in Figure 16(i), the presence of the adhesive is revealed by the peculiar appearance of the air inclusions, in Figure 16(ii) the traces of the adhesive remained entrapped within the peaks induced by laser ablation is apparent mainly due to the different capability to dissipate electric charge.

A further increase of ED resulted in a decline of the failure load which must be differentiated according to the applied ageing method: even if the average value of failure load decreased for every class of joints, the effect of the ageing process was higher over the samples treated with

method (B), for whom the reduction of the failure load ranged from 6.9% (ED=0.51 J/mm^2, H=50 µm) to 18.1% (ED=5.71 J/mm^2), than the ones undergoing method (C), which instead presented a further decrease of the failure load reduction (until 1.4% when ED was equal to 5.71 J/mm^2).

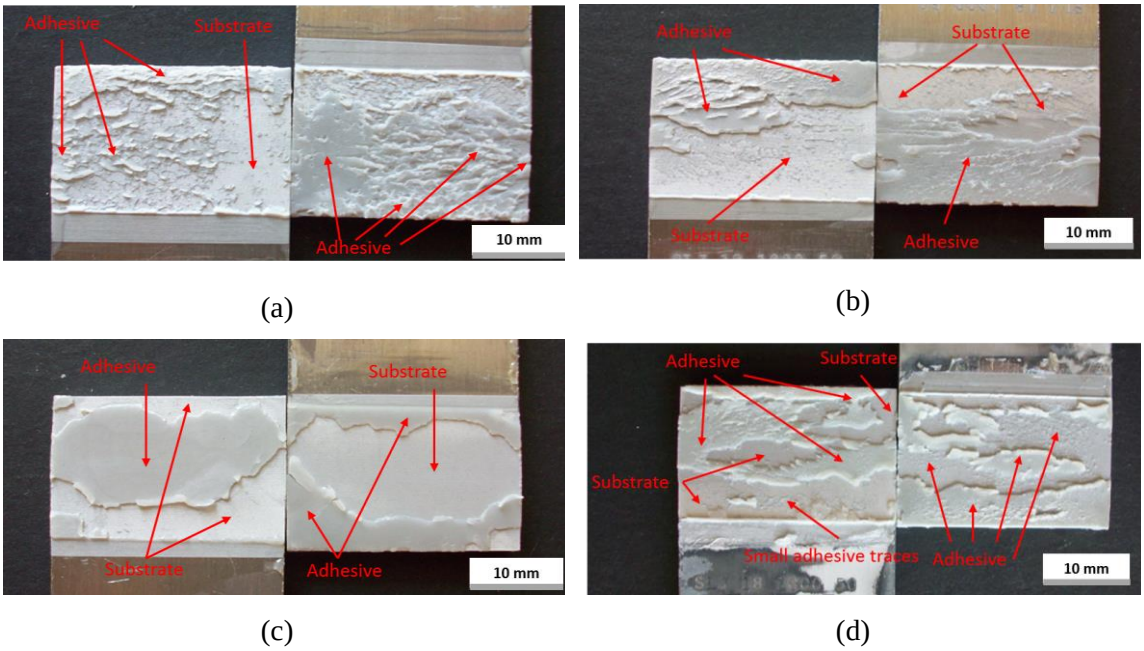

Figure 11 -Photographs showing details of fracture surface of aluminium SLJs pre-treated with laser ablation (ED = 0.51 J/mm^2, H = 50 µm) and subjected to different ageing methods: (a) unaged; (b) method(A); (c) method (B); (d) method (C)

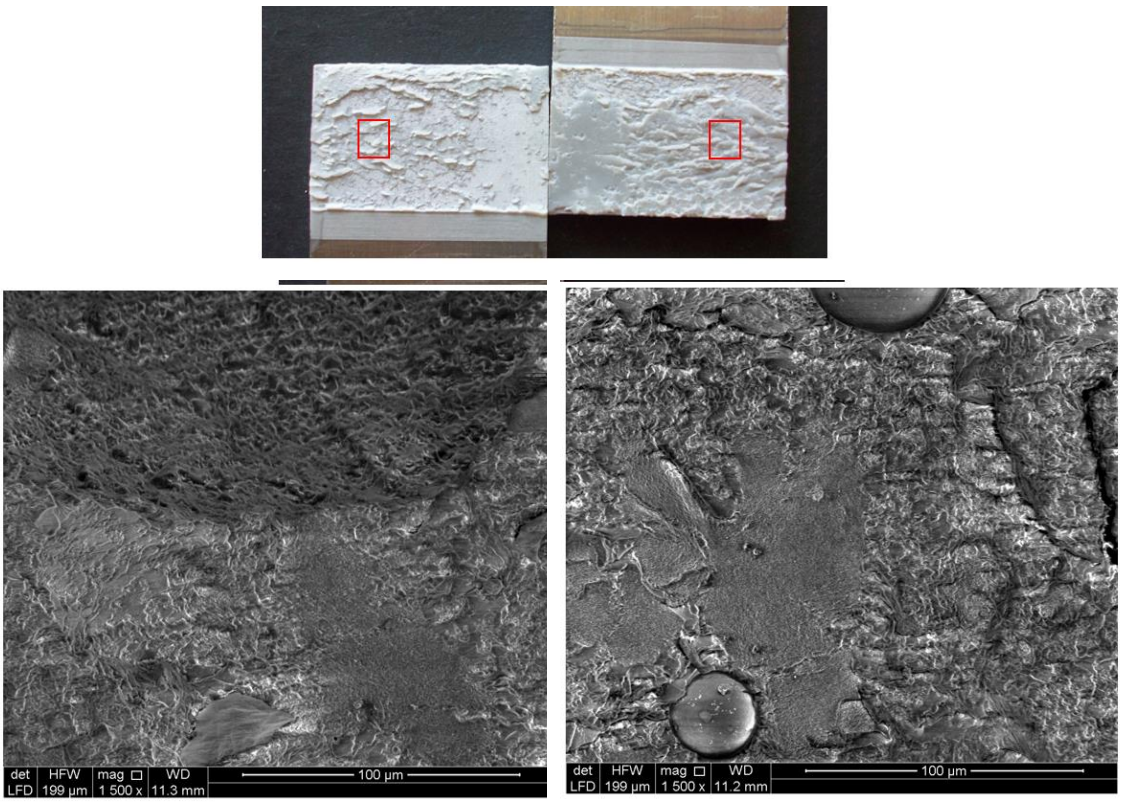

(i) (ii)

Figure 12 - SEM images of fracture surface of laser ablated (ED=0.51 J/mm^2, H=50 µm) unaged aluminum joint((i) left side; (ii) right side)

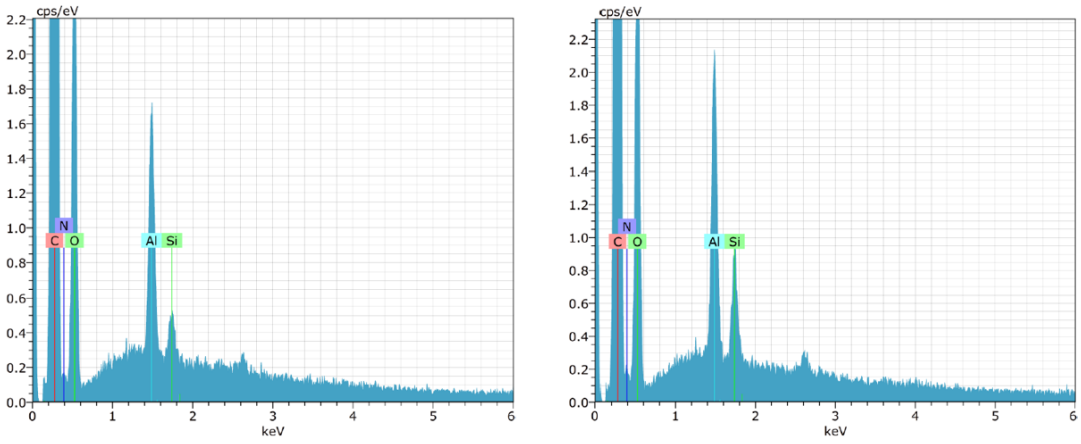

(i) (ii)

Figure 13 - Global EDX spectra measured on the observed surfaces shown in Figure 12(i) and (ii), respectively: the presence of silicum was ascribed to a metallic charge in the adhesive

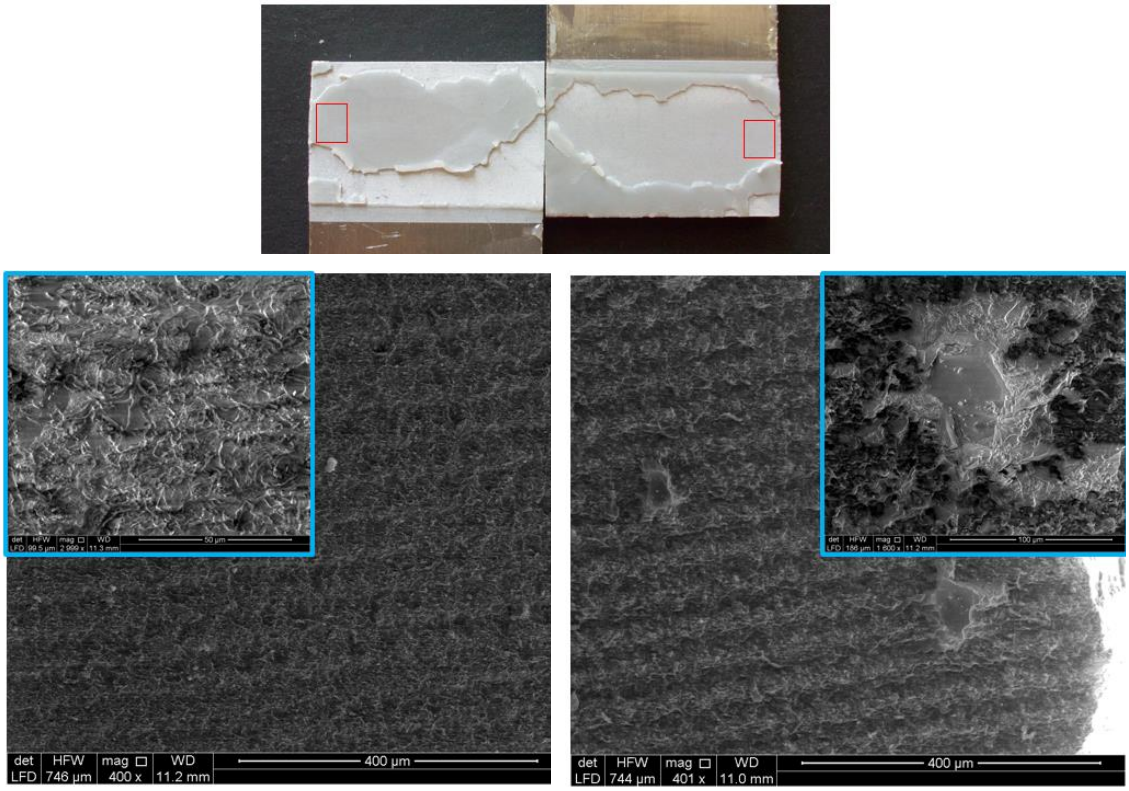

(i) (ii)

Figure 14 - SEM images of laser ablated (ED=0.51 J/mm^2, H=50 µm) aluminum joint subjected to aging method B((i) left side; (ii) right side), with magnified details (in the blue boxes).

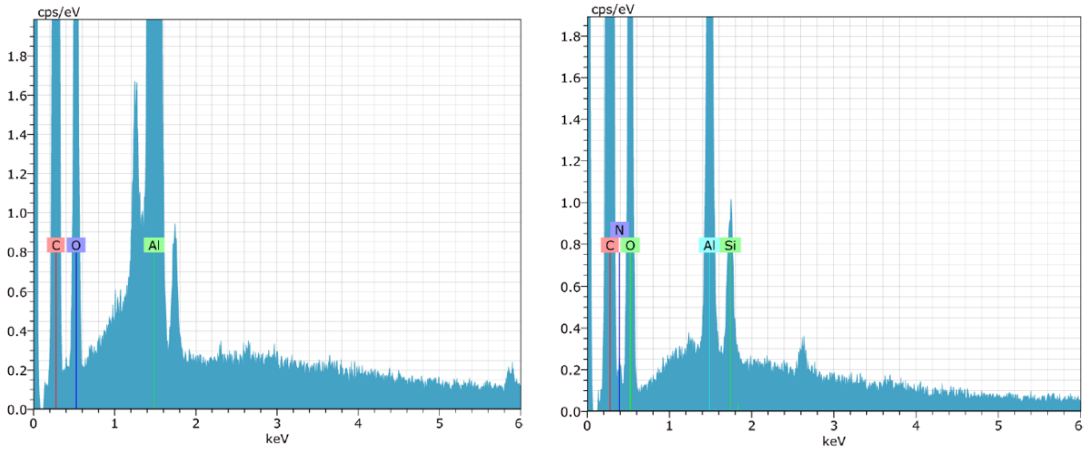

(i) (ii)

Figure 15 - Global EDX spectra measured on the observed surfaces shown in Figure 14(i) and (ii), respectively

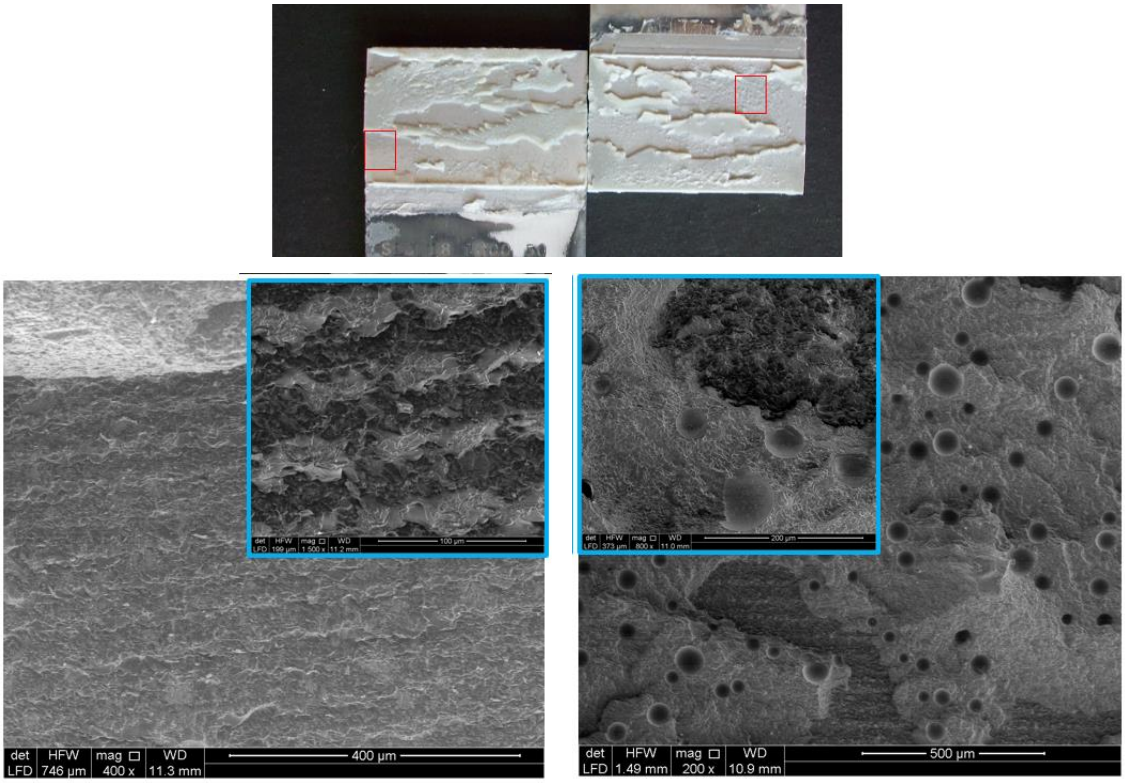

(i) (ii)

Figure 16 - SEM images of laser ablated (ED=0.51 J/mm^2, H=50 µm) aluminum joint subjected to aging method C ((i) left side; (ii) right side), with magnified details (in the blue boxes).

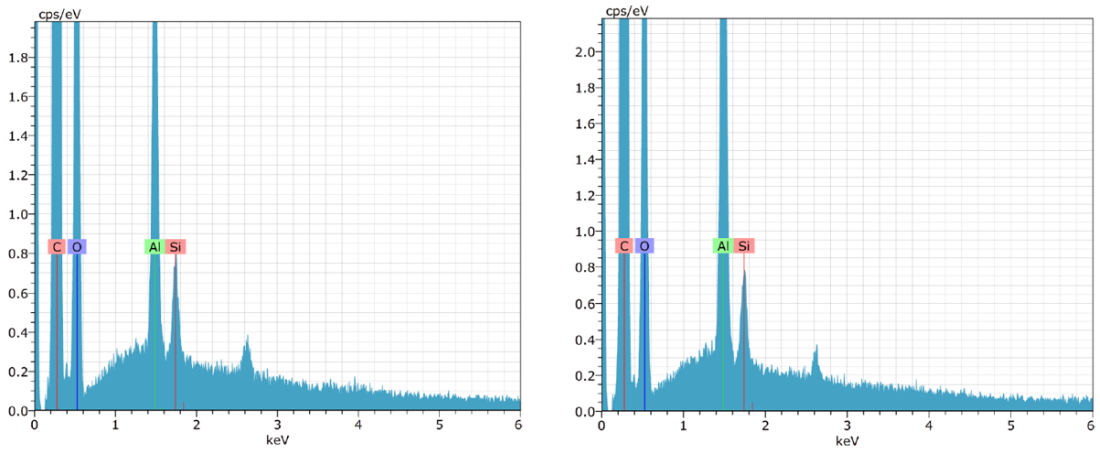

(i) (ii)

Figure 17 - Global EDX spectra measured on the observed surfaces shown in Figure 16(i) and (ii)

Regarding the influence that the hatch distance had over the mechanical response, a laser ablation performed using H = 100 μm resulted in a general increase of the reduction of the failure load, comparing it with the results get with H = 50 μm and by keeping the same value of ED. The associated trend of the failure mode was consistent with the mechanical results, as it is shown in Figure 18. The failure evolved from predominantly cohesive when any ageing was applied (Figure 18 (a)) to an increase of the amount of adhesive detached close to the interface when ageing (A) occurred (Figure 18 (b)), to an apparently interfacial detachment for joints treated with ageing (B) (Figure 18 (c)) and finally to a return of a more winding crack path for samples aged with method (C) (Figure 18 (d)). Even in this case, SEM analysis were carried out to confirm the assumptions. In Figure 19, some portions of the fracture surfaces of the unaged joints of this class of specimens are shown. Although the detection of the imprints left by the laser ablated spot on the adhesive (as a result of the peeling mechanism of failure), many adhesive layers are clearly distinguishable, as a consequence of a crack propagating within the adhesive. EDX spectra (Figure 20) revealed a higher amount of aluminum where the imprints of the laser spots were found, due to the presence of the ablation products, while in the areas where the interface was nearly untouched by the crack propagation the detected amount of aluminum is significantly lower. Moving to the specimen subjected to aging method B, in Figure 21 the differences in the morphology of three different neighboring areas are appreciable on both substrates. In particular, by means of EDX (Figure 22) it is possible to state that the area on which the metallic substrate is barely visible (C) is characterized by poor presence of residual adhesive, while on the polymeric resin some traces of aluminum were however detected, probably because of the ablation process. Finally, on the specimen subjected to aging method C (Figure 23), although with both SEM analysis and EDX measurements, several zones with an interfacial fracture (A and D in Figure 23) were evident, a poor presence of aluminum in other zones of fracture surface indicates that a more cohesive fracture actually occurred.

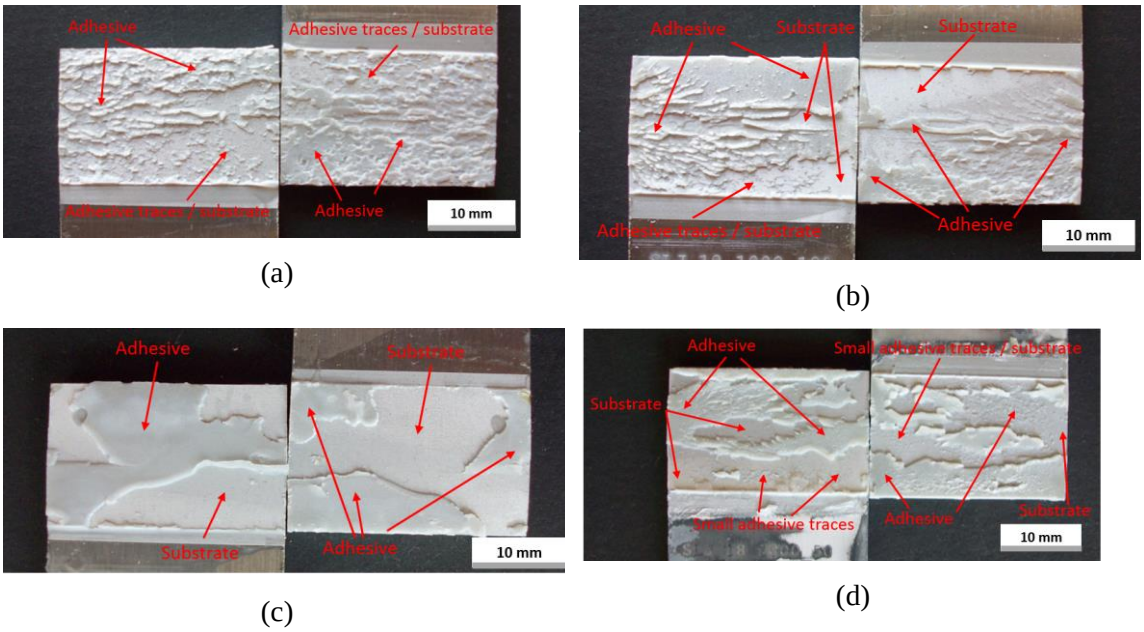

Figure 18 – Photographs showing details of fracture surface of aluminium SLJs pre-treated with laser ablation (ED = 0.51 J/mm^2, H = 100 µm) and subjected to different ageing methods: (a) unaged; (b) method(A); (c) method (B); (d) method (C)

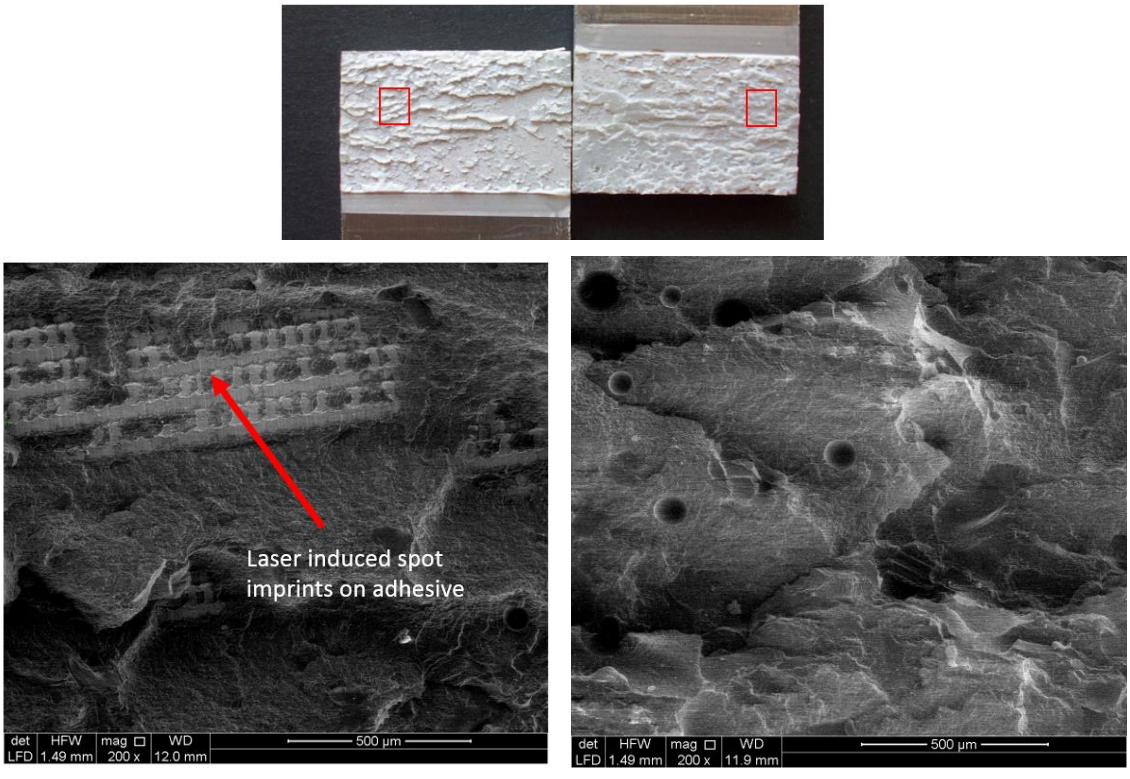

Figure 19 - SEM images of laser ablated (ED=0.51 J/mm^2, H=100 µm) unaged aluminum joint ((i) left side; (ii) right side).

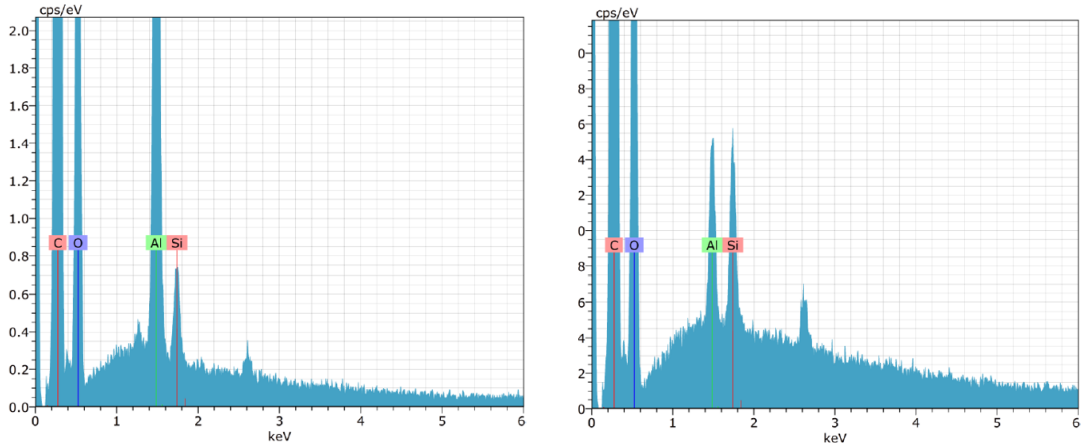

(i) (ii)

Figure 20 - Global EDX spectra measured on the observed surfaces shown in Figure 19(i) and (ii)

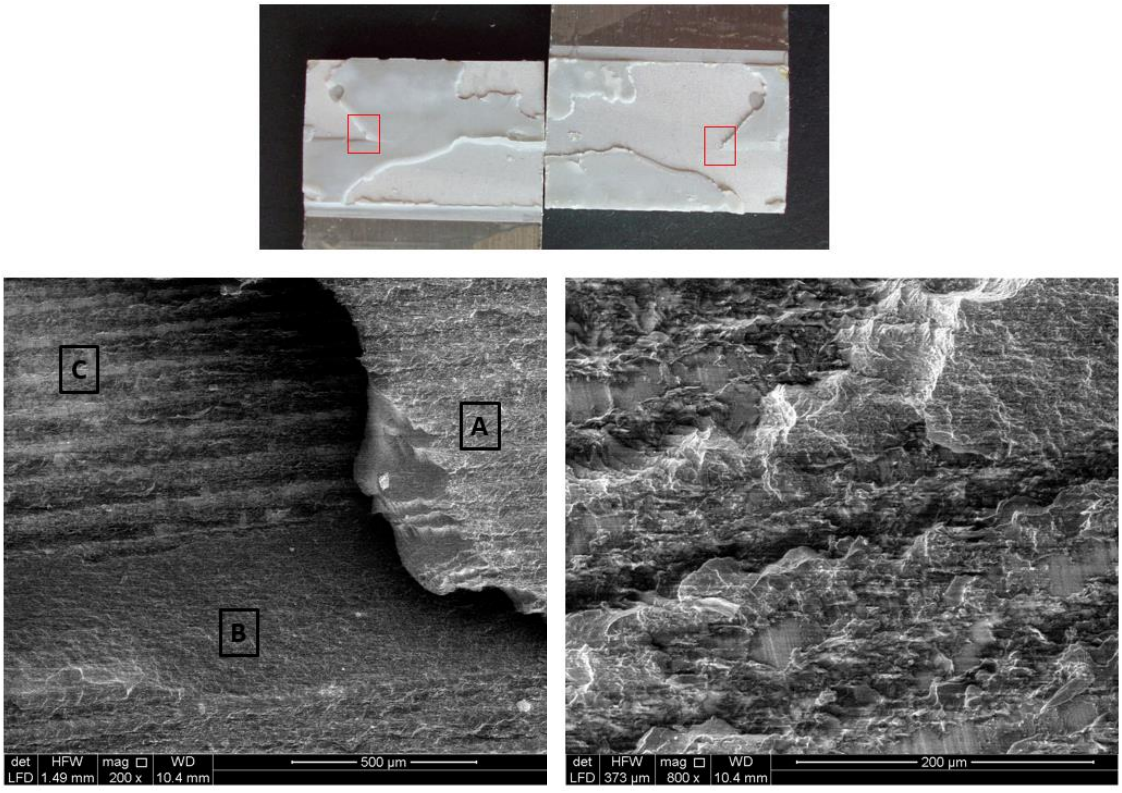

(i) (ii)

Figure 21 - SEM images of laser ablated (ED=0.51 J/mm^2, H=100 µm) aluminum joint subjected to aging method B ((i) left side; (ii) right side).

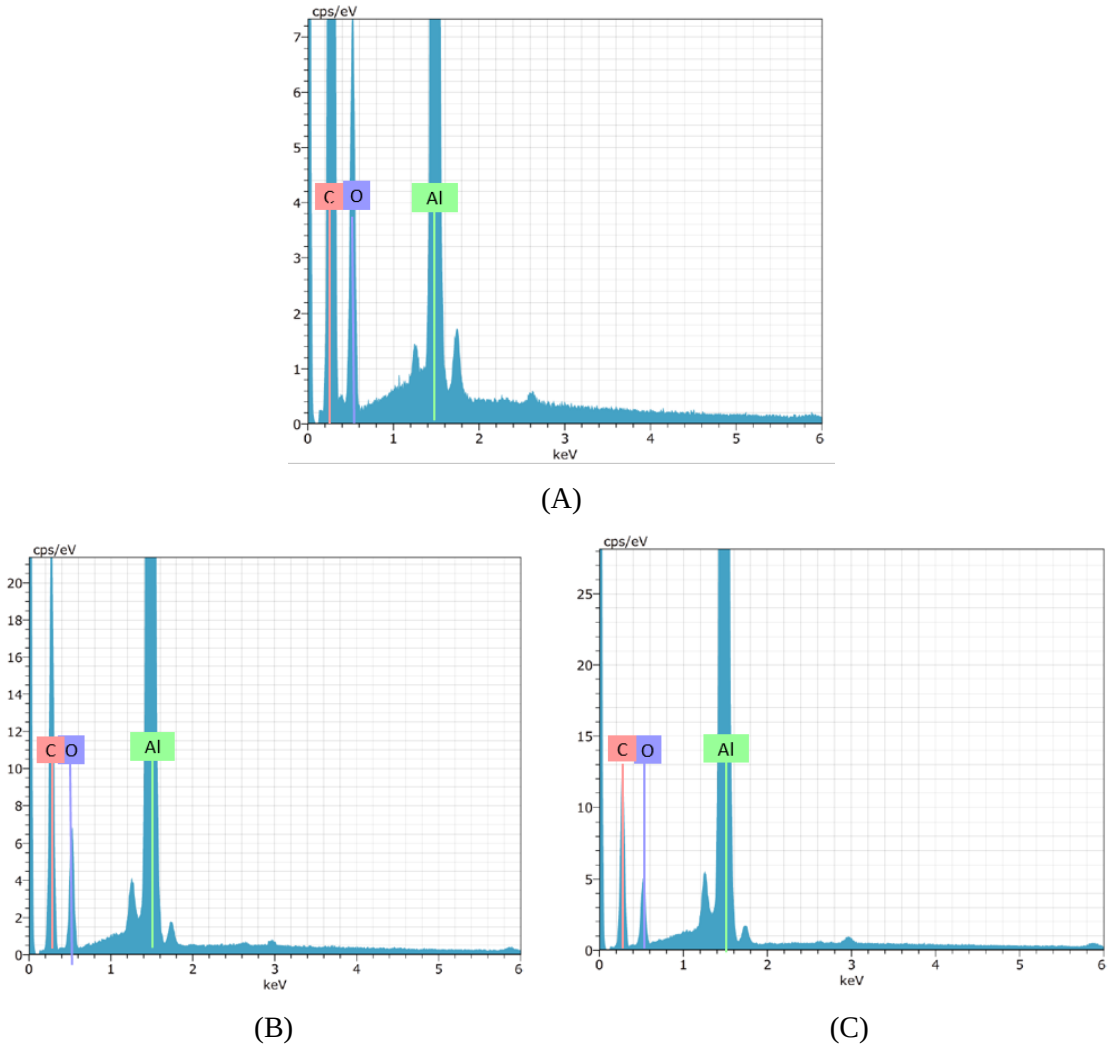

Figure 22 - Local EDX spectra measured on the areas A, B, C, respectively, of the surface shown in Figure 21(i)

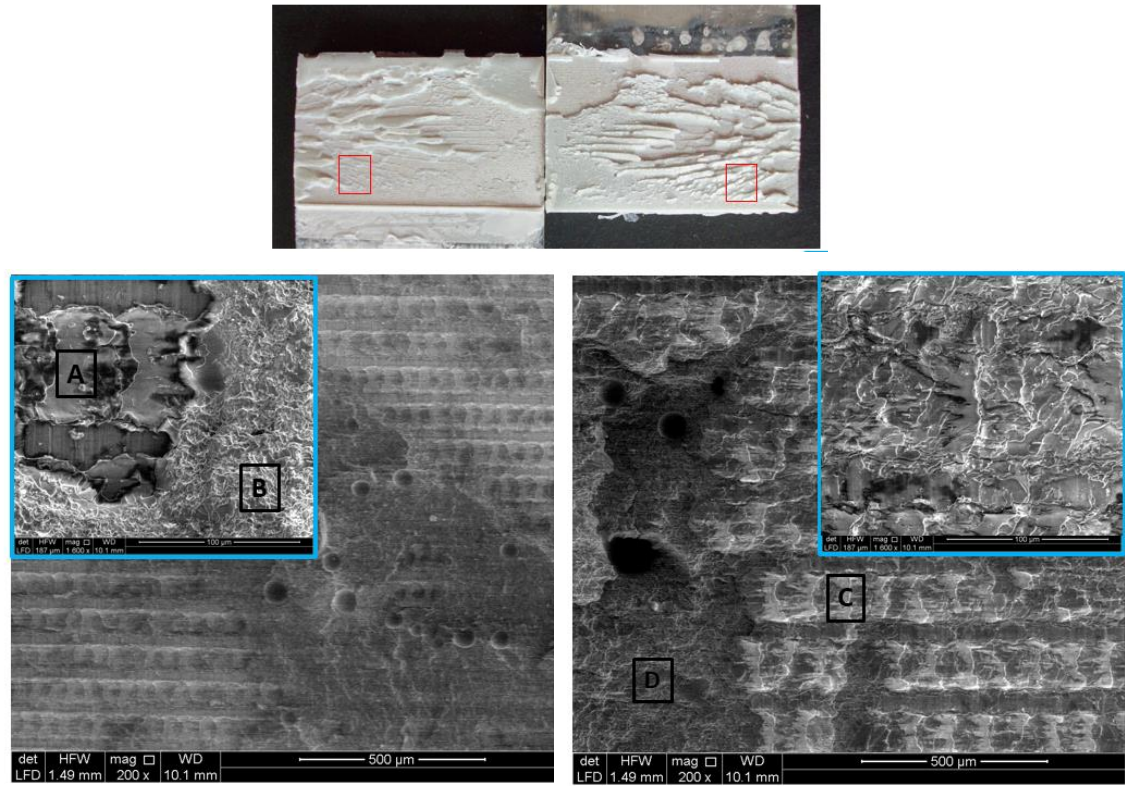

(i) (ii)

Figure 23 - SEM images of laser ablated (ED=0.51 J/mm^2, H=100 µm) aluminum joint subjected to aging method C ((i) left side; (ii) right side), with magnified details (in the blue boxes).

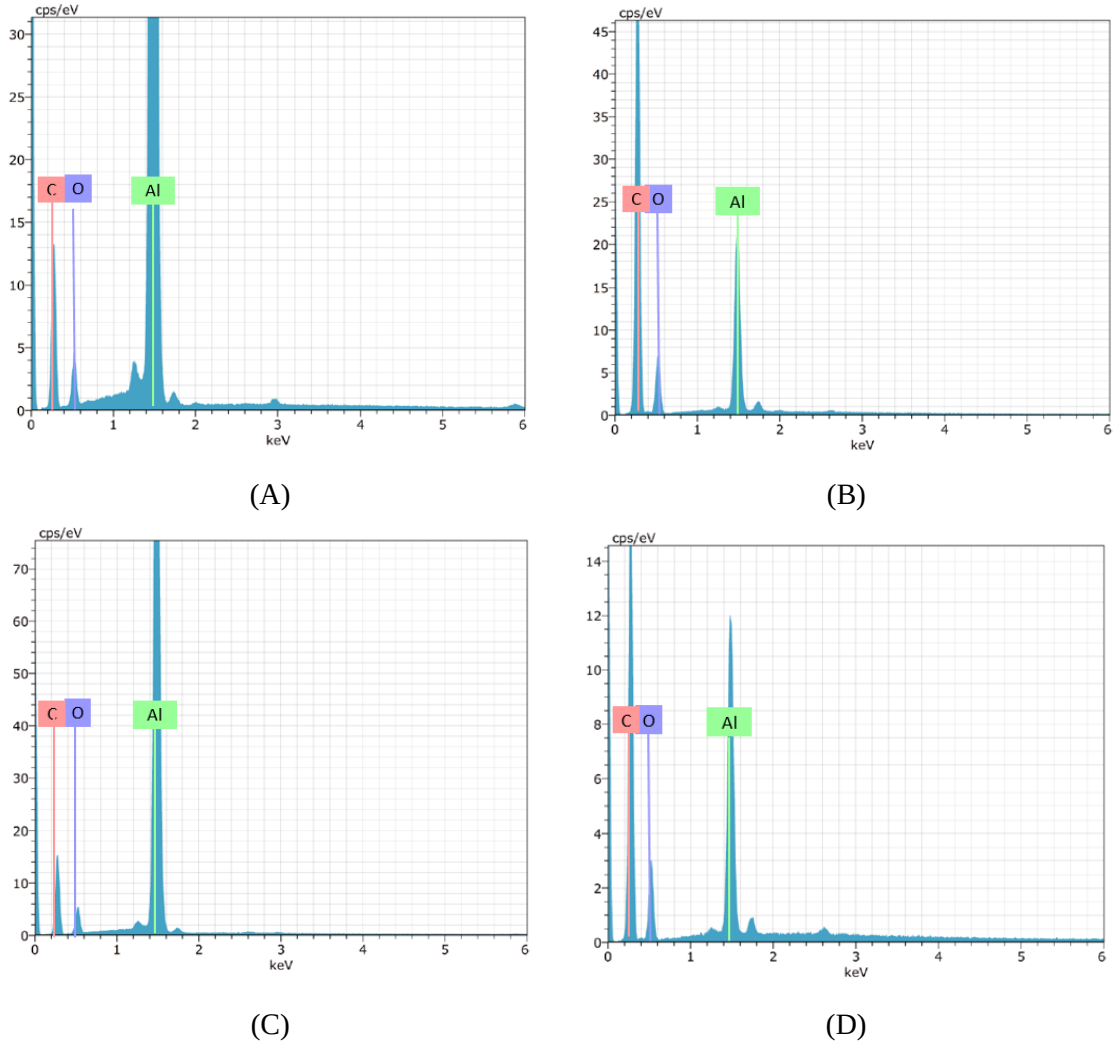

Figure 24 - Local EDX spectra measured on the areas A, B, C, D, respectively, of the surfaces shown in Figure 23

3.2 Stainless steel joints

In Figure 25 the results of the mechanical tests performed over the stainless steel joints are reported. Even in this case, the height of the rectangles represents the mean failure load evaluated from the totality of the tested specimens of a class, while the bars represent the standard deviation. The increase affecting the failure load of the unaged joints recorded from using the simple degreasing to the grit blasting as pre-treatment method, approximately equal to 13.5%, was partially reversed when performing laser ablation with a very low value of ED, capable to produce an improvement only equal to about 5.2%. Then, rising up the level of ED and keeping the hatch distance fixed, higher values of the failure load were reached, until increasing it up to 17% with respect to the degreased samples when ED was equal to 1.14 J/mm^2. Finally, a further increase of ED to 5.71

J/mm^2 produced a decline of the failure load to a level just above (about +8.1% than the average degreased value) the one achieved with ED = 0.17 J/mm^2 (about +5.2% than the average degreased value). The trends of the failure load belonging to the aged specimens were quite similar, with the exception represented by the fact that the peak was reached in correspondence of ED = 0.51 J/mm^2 for every class of specimens undergoing an accelerated ageing cycle. By performing the laser ablation using 100 µm instead of 50 µm as hatch distance value, for ED = 0.51 J/mm^2, a decrease of the failure load by 11% occurred for the unaged joints. On the other hand, when an ageing process was applied the decrease was less remarkable, resulting in a failure load substantially equal (method (B) and (C)) or even slightly higher (method (A)) than the average value belonging to the unaged joints.

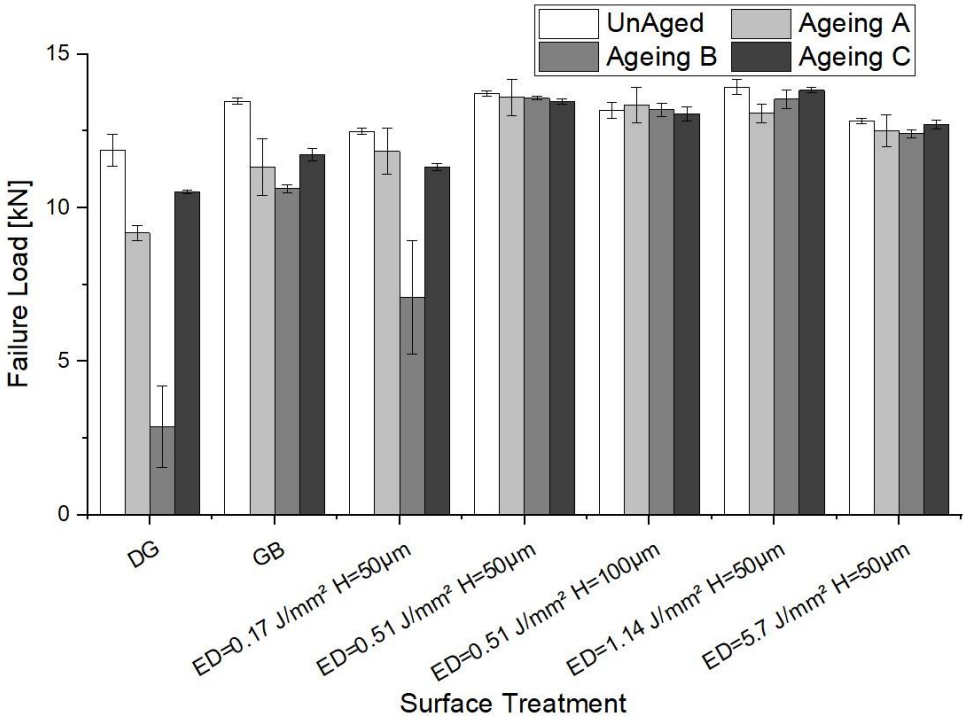

Figure 25 – Effect of the ageing over the failure load of the stainless steel SLJs pre-treated with different methods: degreasing (DG), grit blasting (GB) and laser ablation using several values of energy density (ED) and hatch distance (H).

Even a look at Figure 26, where the average failure load reduction is plotted against the employed pre-treatment for every class of specimens diversified according to the applied ageing process, further enlightens the trends of the failure load. The effect provided by the treatment resulted quite different according to the considered ageing cycle. With refer to the simple degreasing, the samples subjected to method (B) were confirmed to be extremely sensitive to the ageing process, producing a drop of 75.8% of the failure load, while, against what happened in the aluminium joints, method

(C) was the one presenting the lowest decrease of the failure load (-11.4%) with respect to the value of the unaged joints. Instead, when using the grit blasting, although method (B) was associated to the lowest level of failure load, it presented the widest changing of the provided average failure load reduction, which moved from 75% associated to the use of the degreasing to about 20%. This trend was further confirmed by observing the appearance of the fracture surfaces in the four classes of grit blasted specimens, as depicted in Figure 27. While for the unaged specimens (Figure 27(a)) the fracture surface appeared jagged and the crack was forced to cross a path along both the substrates, for all the other classes of samples the failure resulted predominantly adhesive. However, in the specific case of the joints aged with method (B) (Figure 27(c)) the fracture surface appeared smoother than in the other sets, which was consistent with the fact that this class of specimens was the one providing the lowest strength among all the grit blasted joints. The use of the laser ablation led to different results depending from the selected ageing method. Indeed, it seemed to bring benefit to the joints treated with method (A) and (C), while, considering the treatment performed with the lowest available level of ED, the specimens undergoing method (B) appeared to suffer from it and presented a reduction of the failure load equal to 43.2% with respect to the unaged value. This outcome is confirmed by the analysis of the fracture surfaces (Figure 28). From it, the difference in the failure mode occurring between the joints aged with method (B) (Figure 28 (c)), where the fracture resulted apparently interfacial, and the other families of joints (Figure 28 (a)-(b)-(d)), where the detached adhesive resulted scattered in both the substrates, was evident. Limited to this class of specimens, SEM analysis and EDX measurements were acquired in order to better investigate the fracture mode. In Figure 29, the images taken for the case of a joint subjected to aging method (A) are provided. Although in the observed area there is a fairly clear distinction between areas covered with adhesive and zones in which the laser induced spots on the metal substrate are clearly visible, some considerations can be made after evaluating more in detail a single spot. In particular, using high vacuum analysis, on the edge of the spot some traces of adhesive remained mechanically interlocked when the shear load was applied are apparent from their low electrical conducibility. EDX measurements (Figure 30) performed in the middle of the spot (A) and on its edge (B) respectively, confirm this assumption, revealing that in (B) the carbon amount significantly increases with respect to the percentage found in (A). Another EDX measurement on the corresponding side of the other substrate (C) found no relevant traces of Fe over the surface, where the imprints of the laser induced spots are clear. On the joint subjected to aging method (B) (Figure 31), indeed, the correspondence between laser spots on steel and their imprints on the adhesive seems to characterize the whole surface. Again, in this case, the acquisition of EDX spectra shows the presence of traces of adhesive on the edge of the spot (Figure 32) as

documented by the EDX maps where a relevant amount of Fe and C is observed. Finally, in Figure 33 it is possible to appreciate the fracture surface of a joint subjected to aging method C: the same considerations performed for the previous case are still valid. In this case, the EDX map (Figure 34) of a laser induced spot in the metal revealed that the amount of carbon on the edge of the spot is more relevant with respect to the case described in Figure 32 (B). However, an increase of ED from 0.17 J/mm^2 to 0.51 J/mm^2 corresponds to a reduction of the failure load for every class of specimens until values ranging from 0.9% to 1.8%. For example, SEM images acquired on the fracture surface of a laser ablated unaged joint pre-treated with ED=0.51 J/mm^2 are shown in Figure 35. From it, a surface morphology characterized by the indentation of the adhesive within the extremely rough surface produced by laser ablation and the occurrence of mechanical interlock are apparent. The cohesive fracture is confirmed also by EDX acquisition (in A and B in Figure 36) which revealed that the amount of carbon is high even on the substrate where the crack seemed to be propagated closer to the metal/adhesive interface. By increasing ED to 1.14 J/mm^2 and finally to 5.7 J/mm^2, a slight reduction (-6.1% and -2.6%, respectively) of the failure load of the specimens aged with method (A) occurred with respect to the unaged value. On the contrary, the amounts of the average failure load reduction for joints exposed to ageing methods (B) and (C) remained approximately constant to about 3% and about 1%, respectively. Finally, the effect of an increase of the hatch distance to 100 μm seemed to induce a slight reduction of the failure loads with respect to the corresponding results of the H=50 μm, but the inner differences between the aged and the unaged strength values remained below 1%.

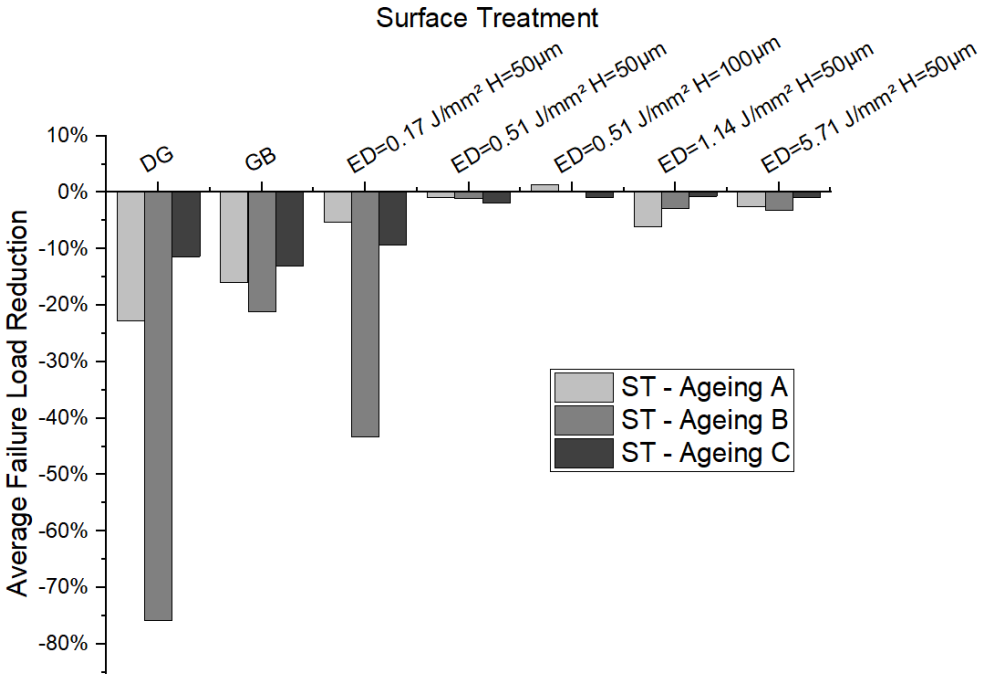

Figure 26 - Influence of the ageing method over the average failure load reduction of stainless steel SLJs, diversified according to the applied pre-treatment

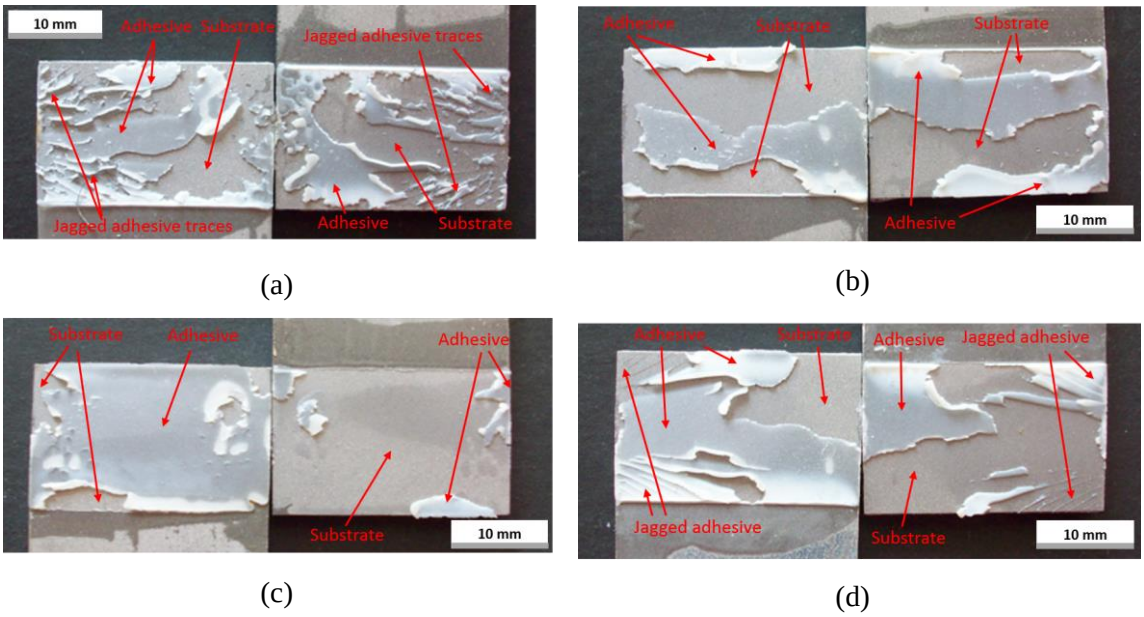

Figure 27 – Photographs showing details of fracture surface of stainless steel SLJs pre-treated with grit blasting and subjected to different ageing methods: (a) unaged; (b) method(A); (c) method (B); (d) method (C)

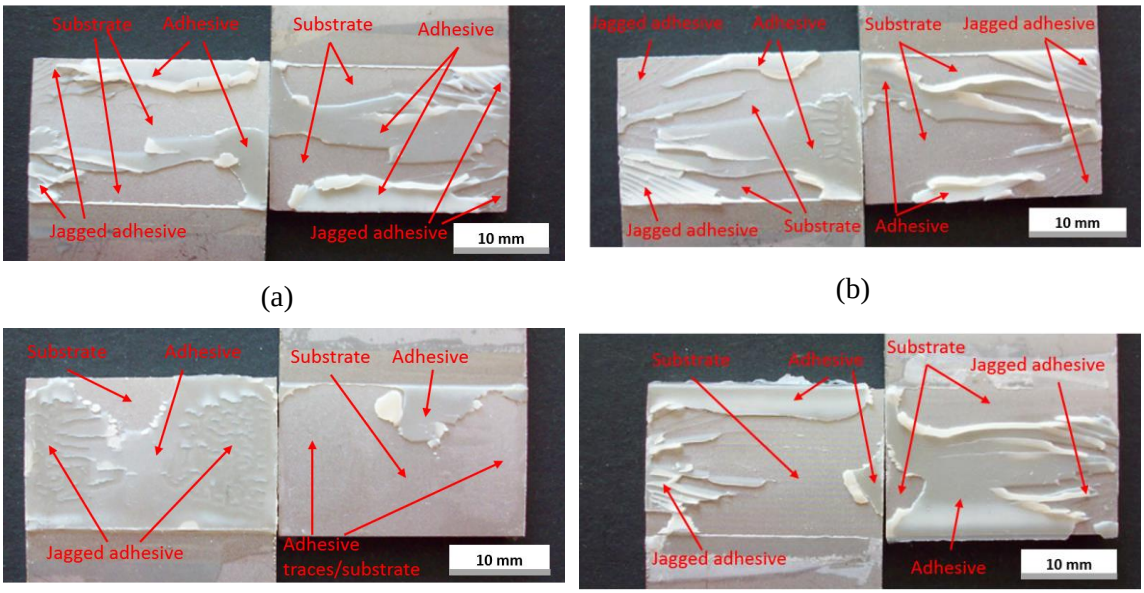

Figure 28 – Photographs showing details of fracture surface of stainless steel SLJs pre-treated with laser ablation (ED = 0.17 J/mm^2, H = 50 µm) and subjected to different ageing methods: (a) unaged; (b) method(A); (c) method (B); (d) method (C)

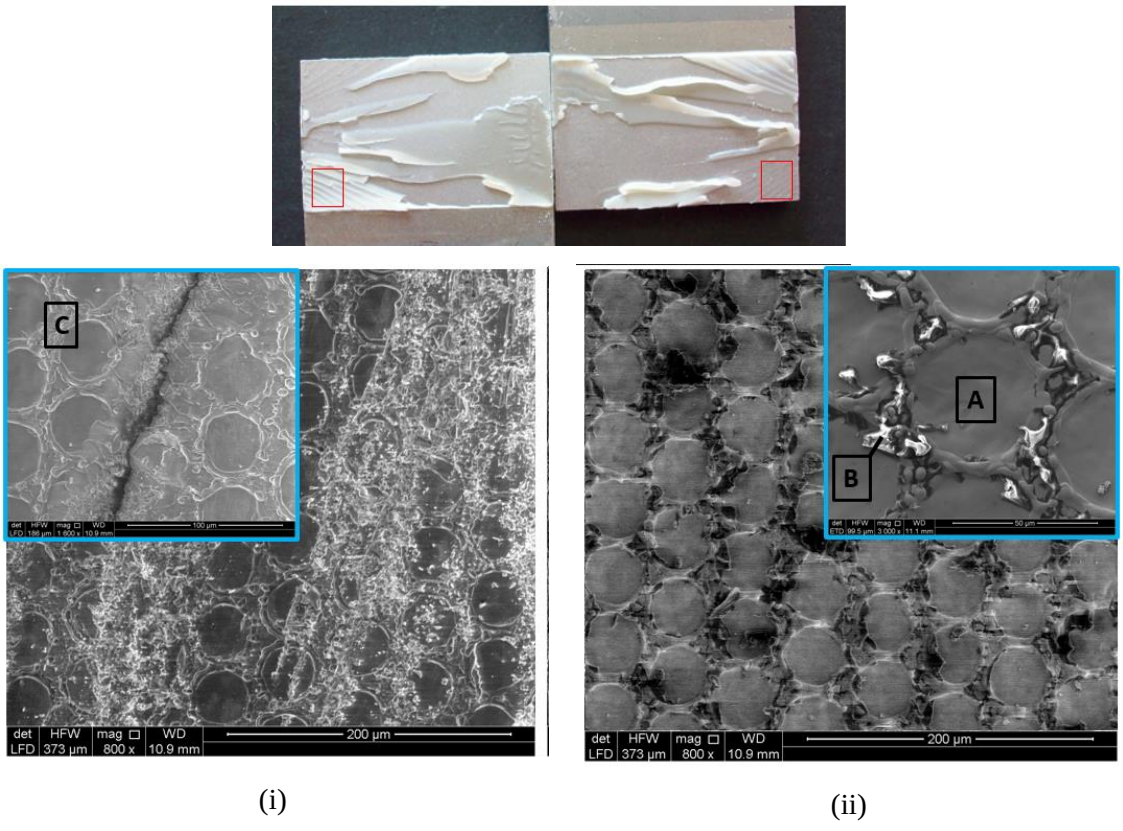

Figure 29 - - SEM images of laser ablated (ED=0.17 J/mm^2, H=50 µm) stainless steel joint subjected to aging method A ((i) left side; (ii) right side), with magnified details (in the blue boxes).

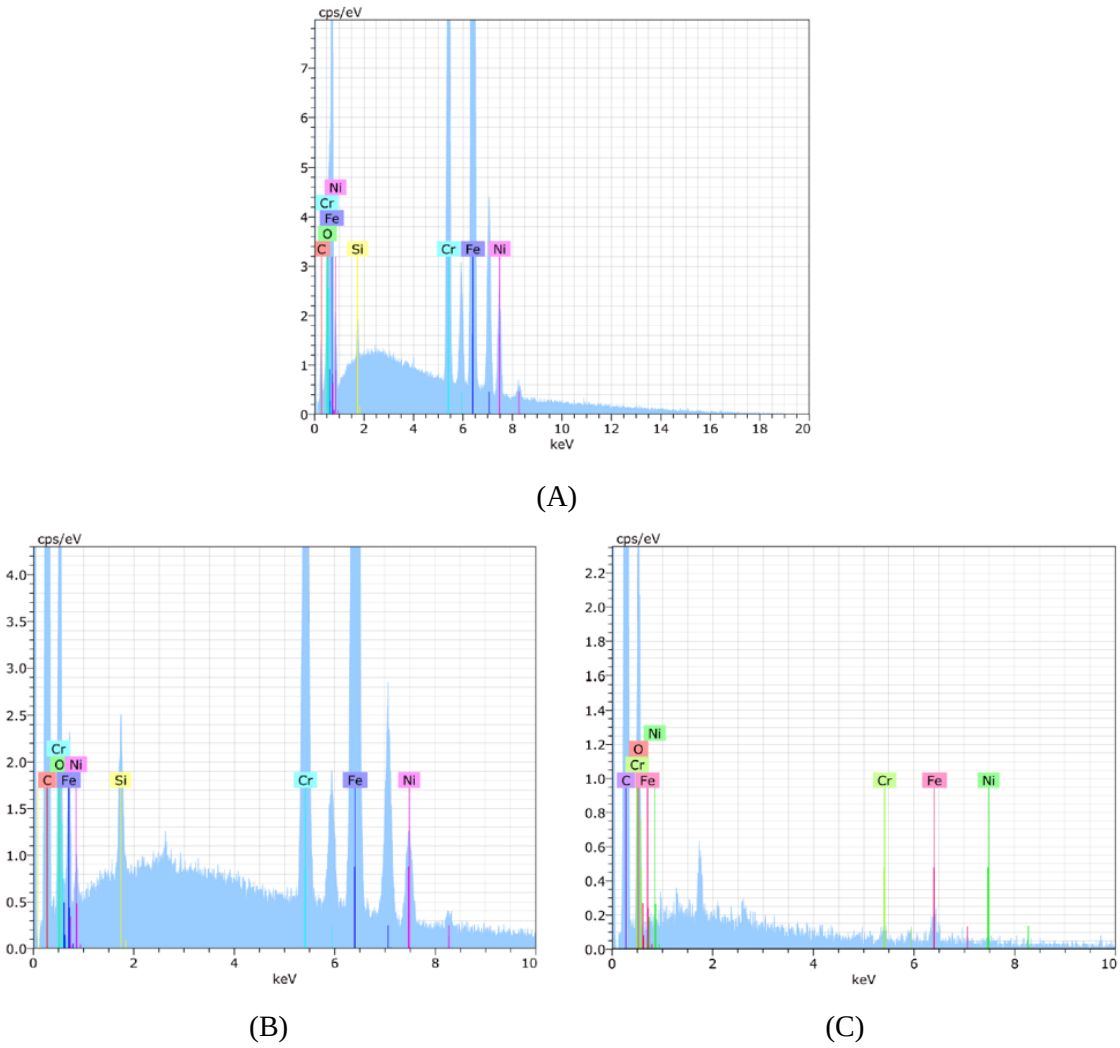

Figure 30 - Local EDX spectra measured on the areas A, B, C, respectively, of the surfaces shown in Figure 29

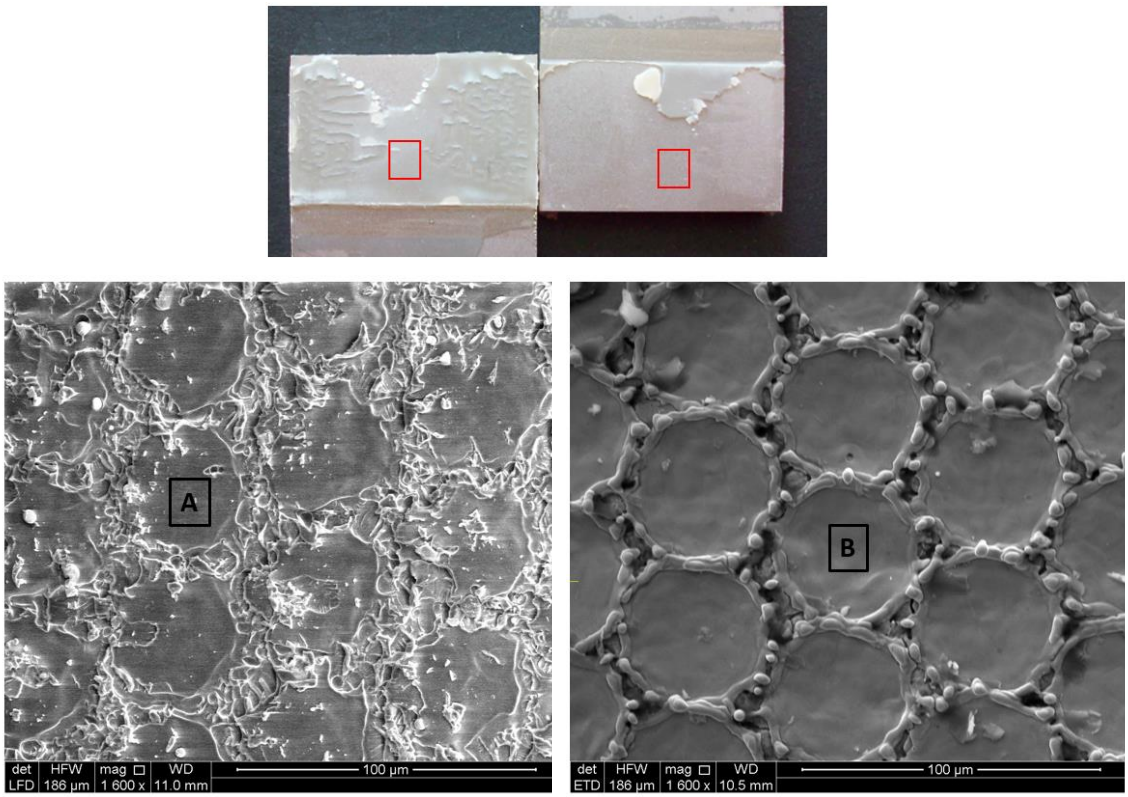

(i) (ii)

Figure 31 - SEM images of laser ablated (ED=0.17 J/mm^2, H=50 µm) stainless steel joint subjected to aging method B ((i) left side; (ii) right side),

A

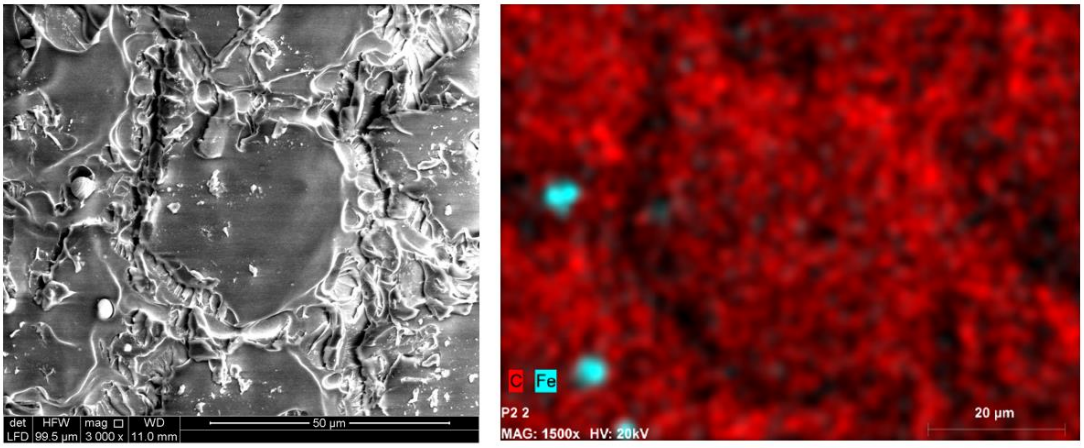

B

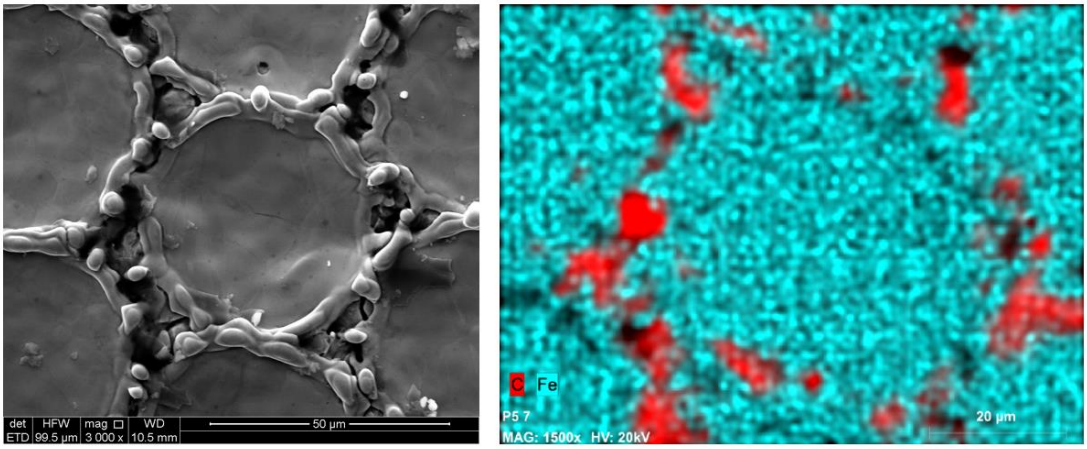

Figure 32 - Local EDX maps of the areas A and B belonging to the surfaces shown in Figure 30

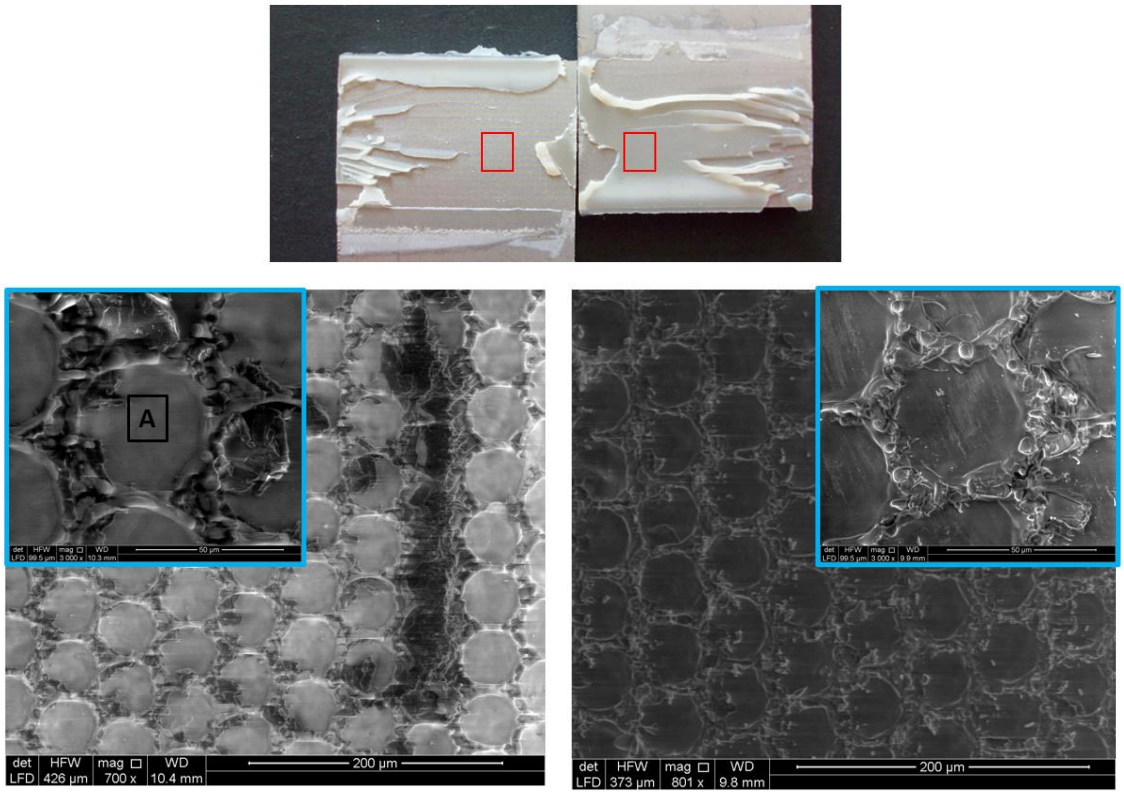

(i) (ii)

Figure 33 - SEM images of laser ablated (ED=0.17 J/mm^2, H=50 µm) stainless steel joint subjected to aging method C((i) left side; (ii) right side),

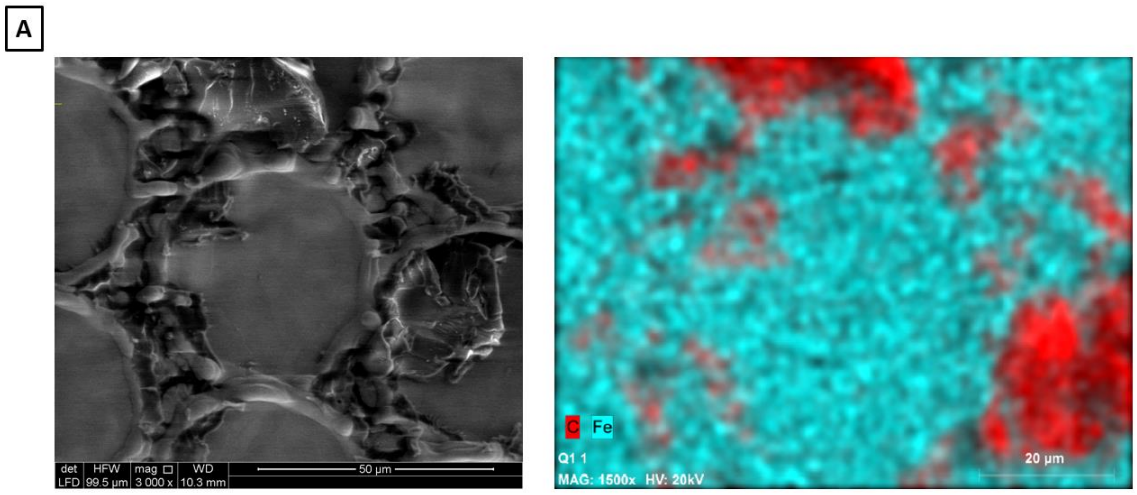

Figure 34 - Local EDX maps of the area A belonging to the surface shown in Figure 32

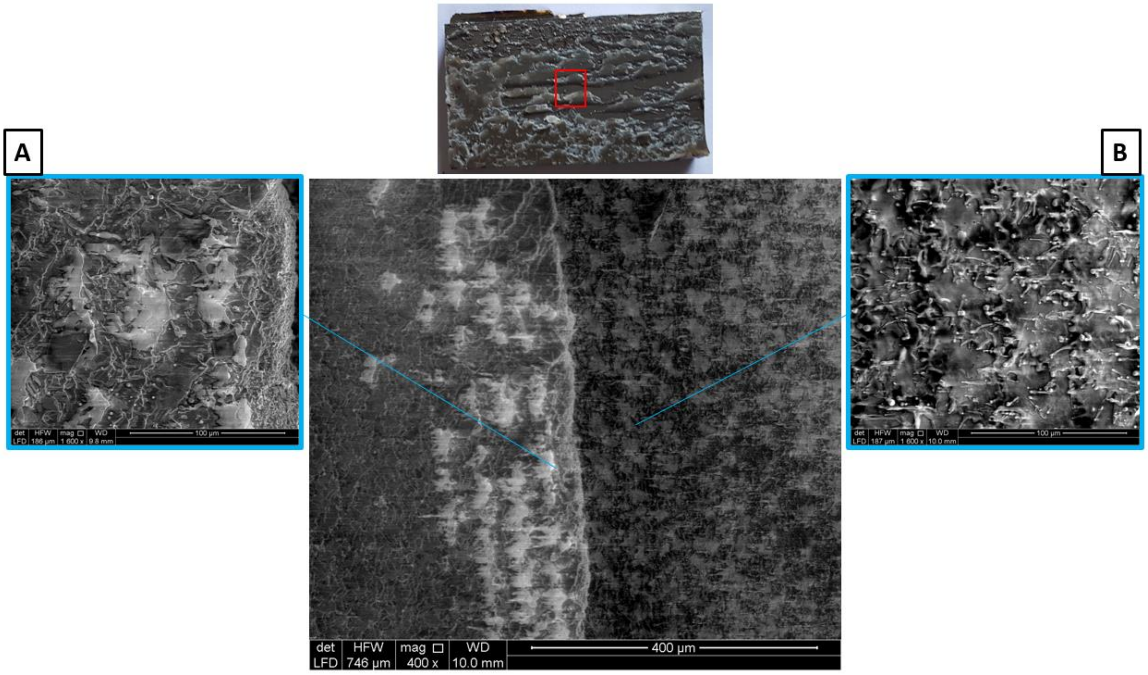

Figure 35 - SEM images of laser ablated (ED=0.51 J/mm^2, H=50 µm) unaged stainless steel joint

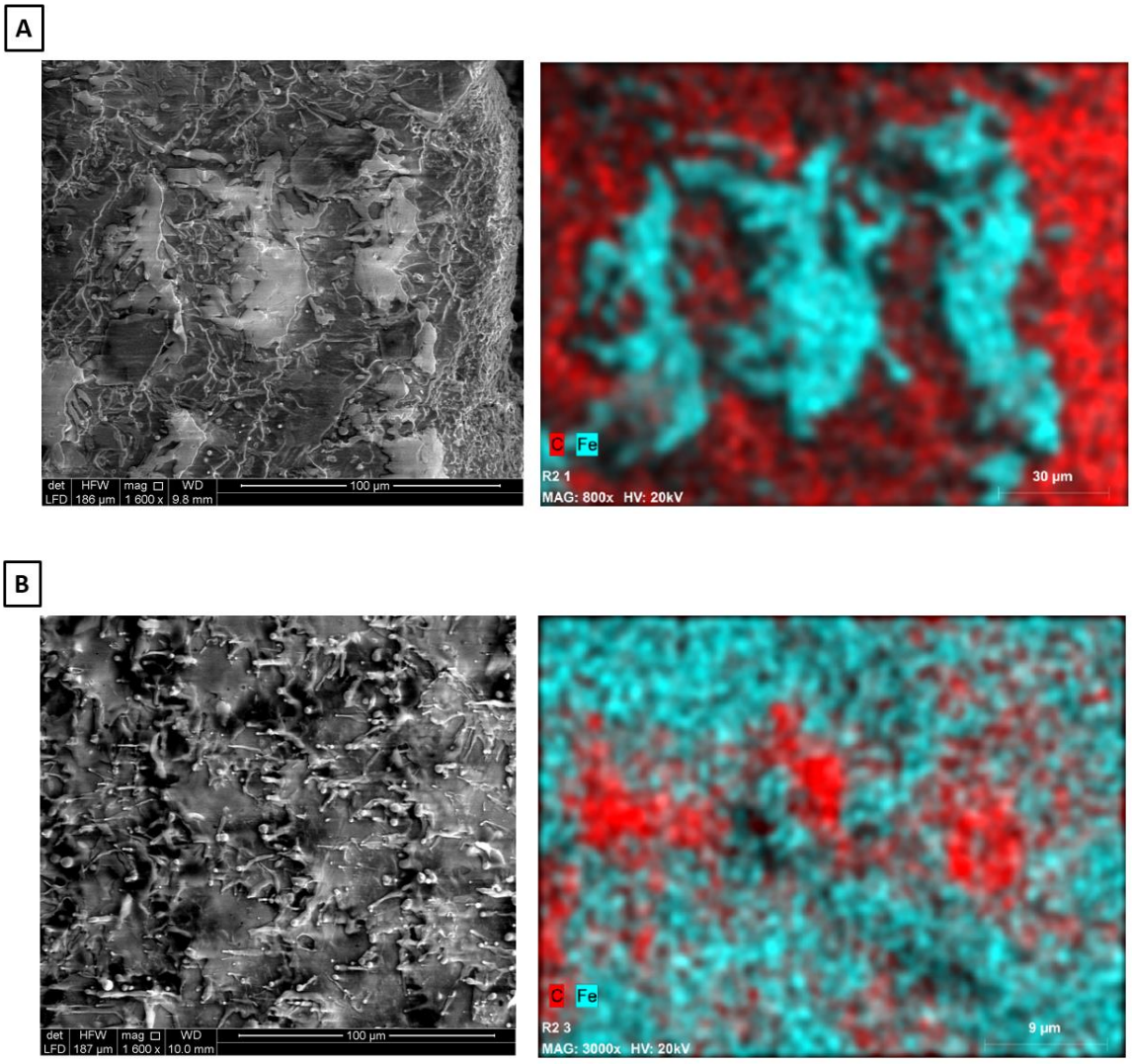

Figure 36 - Local EDX maps on the areas A and B, respectively, belonging to the surface shown in Figure 34

4 Conclusions

In this work, the sensitivity of different techniques used to pre-treat substrates, realized both in aluminium and in stainless steel, of adhesively bonded single lap joints to the occurrence of critical environmental conditions was investigated. The considered pre-treatments were the simple degreasing, the grit blasting and the laser ablation, performed using different combinations of process parameters (power, scan speed, hatch distance) in order to explore a wide range of possible mechanical responses due to the different induced surface morphologies. The onset of ageing was simulated by means of three different methods: a cycle involving temperature and relative humidity

gradients (A) and two immersions into solutions, one alkaline (B) and one acid (C), used for hygienic purposes in the food industry. The changings in the mechanical behavior were assessed through the evaluation of the tensile failure load of the SLJs. For the aluminium joints, the failure load of the unaged joints increased moving from the degreasing to the grit blasting and finally to the laser treatment. The maximum value was reached for laser treatment with the medium low energy density value, after which the failure load gradually returned back to values close to the ones typical of the degreased joints. Apart from the values, the trends exhibited by the failure load of all the aged joints, regardless of the employed method, were analogue to the unaged samples one, but with some inner differences. In particular, while the ageing method (A) did not significantly affect the mechanical strength of the joints, the ageing method (B) resulted very aggressive towards the mechanical properties of the joints, producing a switch of the failure mode from predominantly cohesive to completely adhesive. At the same time, it resulted even very sensitive to the tested pre-treatment, because the amount of reduction of the failure load provided by this environmental exposure progressively decreased from the degreased joints to the grit blasted ones and finally to the laser ablated specimens treated with the threshold value of energy density. With refer to the ageing method (C), it produced a drop of the failure load when the simple degreasing was carried out over the substrate surfaces, while it provided a less perceptible effect over the laser ablated joints. An increase of the hatch distance from 50 to 100 μm produced a lowering of the failure load for all the classes of specimens. The behavior of the unaged stainless steel joints was similar to the one described for the aluminium case, the only exceptions being the fact that the grit blasting showed a higher failure load than the one produced with the lowest energy density laser ablation. All the degreased and the grit blasted specimens considerably suffered from the exposure to an accelerated ageing cycle, especially when method (B) was used. When the laser ablation with the lowest energy density level was employed, the decrease of the failure load for the specimens undergoing ageing methods (A) and (C) with respect to the unaged joints value was lower than the one occurring in the grit blasting case. On the other hand, the samples subjected to ageing (B) were characterized by a further increase of the drop of the failure load with respect to the amount reached with the grit blasting. The sensitivity of the pre-treated specimens to the applied critical environmental conditions completely disappeared when the energy density grew up to the previously identified threshold value, to finally resume (especially for the ageing methods (A) and (B)) with a further increase of the energy density or the hatch distance.

Acknowledgments

This research was supported by the Italian Ministry for University and Research (MIUR), grant SIR RBSI146ZYJ.

References

1. Petrie EM. Handbook of adhesives and sealants. McGraw-Hill; 2000.
2. Poole P, Watts J. Effect of alloy composition and surface pretreatment on the durability of adhesive-bonded aluminium alloy joints. Int J Adhes Adhes 1985;5(1): 33-39.
3. Bijlmer P, Schliekelmann R. The relation of surface condition after pretreatment to bondability of aluminium alloys. SAMPE Quaterly 1973;5:13-27.
4. Digby R, Packam D. Pretreatment of aluminium: topography, surface chemistry and adhesive bond durability. Int J Adhes Adhes 1995;15(2):61-71.
5. Russell W, Garnis E. A chromate-free low toxicity method of preparing aluminum surfaces for adhesive bonding. SAMPE Journal 1981;17:19-23.
6. Minford J. Etching and anodizing pretreatments and aluminum joint durability. SAMPE Quaterly 1978;9:18-27.
7. Hennemann QD, Brockmann W. Surface morphology and its influence on adhesion. J Adhes 1981;12(4):297-315.
8. Harris A, Beevers A. The effects of grit-blasting on surface properties for adhesion. Int J Adhes Adhes 1999;19(6):445-452.
9. Minford J. Durability of structural adhesive bonded aluminum joints. Adhes Age 1978;21(3):17-23.
10. Bishopp J, Sim E, Thompson G, Wood G. Effects of the environment on bonded aluminium joints: an examination by electron microscopy."Adhesion 13". Springer 1989;201-220.
11. Pike R, Patarini V, Zatorski R, Lamm F. Plasma-sprayed coatings as adherend surface pretreatments. Int J Adhes Adhes 1992;12(4):227-231.
12. Kinloch A. Interfacial fracture mechanical aspects of adhesive bonded joints – a review. J Adhes 1979;10(3):193-219.
13. Zheng R, Lin JP, Wang PC, Wu YR. Effect of hot-humid exposure on static strength of adhesive-bonded aluminum alloys. Defence Technology 2015;11(3):220-228.
14. Critchlow G, Brewis D. Review of surface pretreatments for aluminium alloys. Int J Adhes Adhes 1996;16(4):255-275.
15. Butt R, Cotter J. The effect of high humidity on the dynamic mechanical properties and thermal transitions of an epoxy-polyamide adhesive. J Adhes 1976;8(1): 11-19.
16. Costa M, Viana G, da Silva L, Campilho R. Effect of humidity on the mechanical properties of adhesively bonded aluminium joints. Proc IMechE, Part L: J Materials: Design and Applications 2018;232(9):733-742.
17. Viana G, Costa M, Banea M, da Silva L. Behaviour of environmentally degraded epoxy adhesives as a function of temperature. J Adhes 2017;93(1-2):95-112.
18. Rechner R, Jansen I, Beyer E. Influence on the strength and ageing resistance of aluminium joints by laser pre-treatment and surface modification. Int J Adhes Adhes 2010;30(7):595-601.
19. Wu Y, Lin J, Carlson BE, Lu P, Balogh MP, Irish NP, Mei Y. Effect of laser ablation surface treatment on performance of adhesive -bonded aluminum alloys. Surf Coat Technol 2016;304:340-347.

20. Musiari F, Moroni F, Favi C, Pirondi A. Durability assessment of laser treated aluminium bonded joints. Int J Adhes Adhes 2019;93:64-75;doi: 10.1016/j.ijadhadh.2019.01.017
21. Moroni F, Musiari F, Romoli L, Pirondi A. Influence of laser treatment parameters on the mode I strain energy release rate of aluminium double cantilever beam joints. Int J Adhes Adhes 2018;83:31-40; doi.org/10.1016/j.ijadhadh.2018.02.023
22. Adams RD. Adhesive bonding: Science, technology and applications. England: Woodhead publishing Ltd; 2000
23. Kothe C, Rudolph L, Weller B, Wünsch J. Investigations on the ageing resistance of sealing materials for the protection of bonded point fixings. Conference proceedings of "Glass performance days 2015" held in Tampere, Finland, June 24-26, 2015, pp 278-280
24. Hildebrand J, Werner F. Glass-plastic hybrid construction. Advances in Engineering structures, mechanics & construction – Proceedings of an International conference on Advances in Engineering Structures, Mechanics & Construction, held in Waterloo, Ontario, Canada, May 14-17, 2006, editors: M. Pandey, W. Xie, L. Xu, pp 801-808